

Monte Carlo Investigation of a Model Hamiltonian Including Splay-distortion and Polar Interactions

A Dissertation submitted to the University of Hyderabad
in partial fulfilment of degree of

MASTER OF TECHNOLOGY

in

COMPUTATIONAL TECHNIQUES

by

VIJAY KUMAR GUDELLI



School of Physics
University of Hyderabad
(P.O) Central University, Gachibowli
Hyderabad 500 046
Andhra Pradesh
India

To

MY Parents and Family



DECLARATION

I **VIJAY KUMAR GUDELLI** hereby declare that this Dissertation entitled “Monte Carlo Investigation of a model Hamiltonian including Splay-distortion and Polar interactions” submitted by me under the guidance and supervision of **Prof. V.S.S.SASTRY** is a bonafide work. I also declare that it has not been submitted previously in part or in full to this University or any other University or Institution for the award of any degree or diploma.

Date:

Place:

VIJAY KUMAR GUDELLI



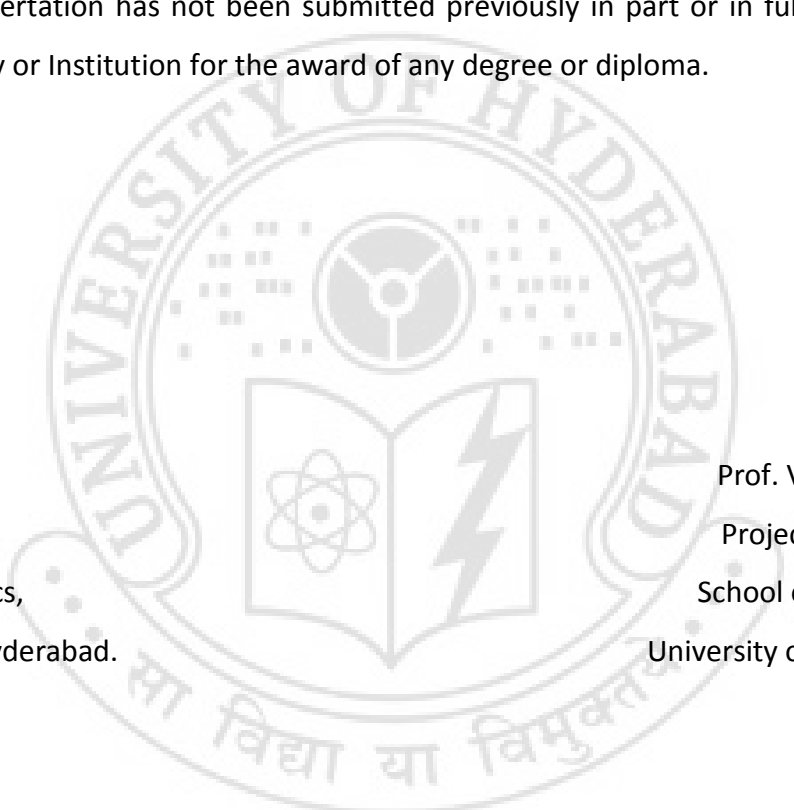
CERTIFICATE

This is to certify that the dissertation entitled “Monte Carlo Investigation of a Model Hamiltonian Including Splay-distortion and Polar Interactions” submitted by VIJAY KUMAR GUDELLI bearing Reg. No. 09PCMT05 in partial fulfilment of the requirements for the award of the degree of Master of Technology in Computational Techniques, is a bonafide work carried out by him under my supervision and guidance.

The dissertation has not been submitted previously in part or in full to this or any other University or Institution for the award of any degree or diploma.

Dean
Prof. C. Bansal,
School of Physics,
University of Hyderabad.

Prof. V.S.S.Sastry
Project Supervisor,
School of Physics,
University of Hyderabad.



Preface

The model Hamiltonian proposed recently for studying splay-induced flexoelectric effects the relative influences of the polar ordering term (B) and splay distortion energy (C) on the phase diagram, as function of temperature and external field. The observations reported earlier based on the lattice model considered two combinations of these parameters and their thermal behaviour was simulated based on Monte Carlo methods. It was observed that with appropriate choice of B and C terms it was possible to induce a splay transition, and even a simultaneous thermally induced transition of nematic polar and splay orders. In this context this model Hamiltonian looked very interesting and promising. This distortion reports our observations based on Monte Carlo simulation of manifestation of this model.

In this context we studied the liquid crystal systems with a suitable lattice based Hamiltonian, using Metropolis algorithm based Monte Carlo simulations and we restricted the interactions to only the nearest neighbours (Lebwohl-Lasher model) for a $10 \times 10 \times 10$ cubic system. The objective of the present work is to explore the sub space of these few parameters to examine the relative effects of polar ordering term and the splay interaction term, we varied B from 0.1 to 0.9 in steps of 0.2, and similarly C has been varied for each of these B values again from 0.1 to 0.9 in steps of 0.2, and also supplement this subspace of (B, C) parameters with certain choice values for no splay contribution, we examined a of total 30 sets of [B, C] pairs for different temperature values. The computed thermal averages in each case include the orientational order parameter S, the polar order parameter P, the splay order parameter θ , the specific heat (at constant volume) C_V , the variance in the equilibrium fluctuations in S (χ_S), and those in P (χ_P). Finally we also observed that the splay transition predicted from this model based on earlier Monte Carlo simulations could not be seen in the present study, nor could the simultaneous transition of nematic, polar and splay orders be verified.

Contents

Page No.

1. Introduction	
1.0 Introduction to Liquid Crystals.....	6
1.1 Classification of Liquid Crystal Phases.....	7
1.2 Order Parameter.....	12
1.3 Introduction to Flexoelectric effect in liquid crystals.....	12
2. Monte Carlo study of the flexoelectric Hamiltonian	
2.0 Need of Computer Simulation.....	17
2.1 Monte Carlo Simulation.....	19
2.2 Metropolis Algorithm.....	20
2.3 Physical Systems.....	22
2.4 Effect of parameters used in the Hamiltonian.....	23
2.5 Discussion.....	62
3. Conclusion.....	65
Bibliography.....	67

Chapter 1:

INTRODUCTION

1.0 Introduction to Liquid Crystals:

For many years matter was thought to exist in three phases: solid, liquid, and gas. But this scenario is not correct exactly. Some of the materials like certain organic compounds exhibit intermediate phases in between crystalline solids and liquids on heating. This intermediate phase behaves mostly like crystalline solids, But with certain aspects of liquids. For example, in a crystal the molecules are located at regular points in space; this will follow a translational order, whereas in a liquid this translational ordering of molecules does not exist. For this reason these intermediate phases are named liquid crystalline phases, or mesomorphic phases (mesophases).

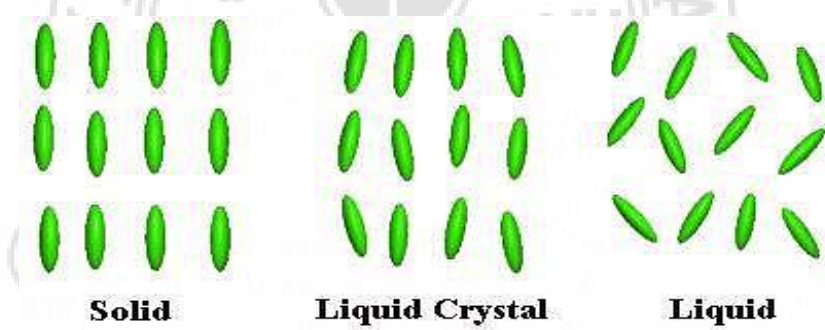


Fig.1.1 Schematic molecular arrangement in matter.

The mesophases were first observed by an Austrian botanist named Friedrich Reinitzer in 1888 [1], that material like cholesteryl benzoate had two distinct melting points, at the first the crystal melted into a cloudy liquid and at the second the liquid became clear transparent liquid. Later in 1889 this new kind of state of matter is named as Liquid Crystalline phase by Lehmann.

Liquid crystal materials are unique in their properties and uses. These will also possess some of the properties of crystalline solids and isotropic liquids. For example mechanical properties liquids like fluidity, inability to support shear formation and coalescence if droplets are also exhibited by the mesophase and crystalline properties like

anisotropy in their optical, electrical and magnetical properties are also exhibited by the mesophases. So liquid crystals exhibit properties of both crystalline solids and liquids in some aspects.

1.1 Classification of Liquid Crystal Phases:

Liquid crystals are classified as Thermotropic and Lyotropic liquid crystals. In Thermotropic liquid crystals, the shape of the molecule dictates the orientational order and the thermal motion gives the mobility. Thermotropic liquid crystals can generally be formed by prolate (calamitic) molecules or oblate (discotic) molecules. Lyotropic liquid crystals that appear in nature in living organisms acquire mobility by the addition of a solvent and their liquid crystalline properties are governed by the relative concentration of the solute. Lyotropic liquid crystal phases are formed by amphiphilic molecules. However this classification among the Liquid Crystals is not unique and there are materials which exhibit both Thermotropic and Lyotropic crystalline properties are known as Amphotropic.

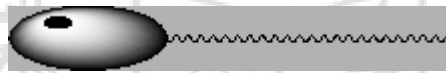


Fig 1.2(a) Schematic diagram of an amphiphilic molecule

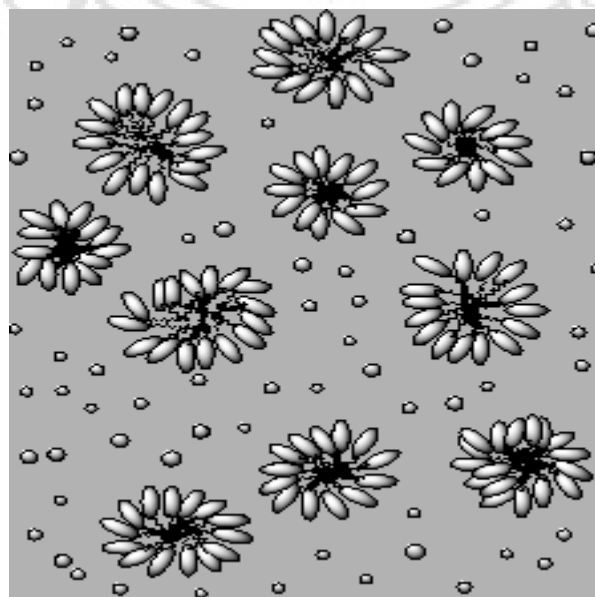


Fig.1.2 (b) Schematic diagram of micelles

Liquid crystals are found in several organic compounds. The organic compounds may be a variety of chemical types such as acids, azo—or azoxy-compounds and cholesterol esters. Typical examples are: molecular structures of para-azoxyanisole (PAA) and p, p-methoxybenzylidene n-butylaniline (MBBA):

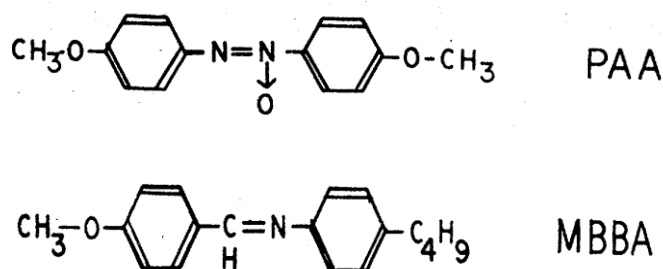


Fig.1.3 Schematic diagram for PAA and MBBA.

The parameters which describe the classification of liquid crystalline structure are: positional order, orientation order and bond order. Positional order refers to the extent to which an average molecule or group of molecules shows translational symmetry. Orientational order, as discussed above, represents a measure of the tendency of the molecules to align along the director on a long-range basis. Bond orientational order describes a line joining the centres of nearest-neighbour molecules without requiring a regular spacing along that line. Based on the parameters described above classification of liquid crystal phases was first given by George Friedel [2].

1.1.1 Nematic Liquid Crystal Phase:

By reducing the temperature from a high value to a low value the isotropic phase, in which the position and orientation of the molecules are random, changes to a nematic phase in which the orientation of the molecules gain some order but not the long-range position order. The molecules can still move around in the fluid, but their orientation remains the same. Molecules in a nematic phase spontaneously order with long axes roughly parallel. The average direction of the molecules is called the director \mathbf{n} which is a

unit vector. The positions of the each molecule prefer to orient along long axis \mathbf{n} , which can be described as $\hat{\mathbf{n}}(\mathbf{r})$ for a r^{th} site in the system.

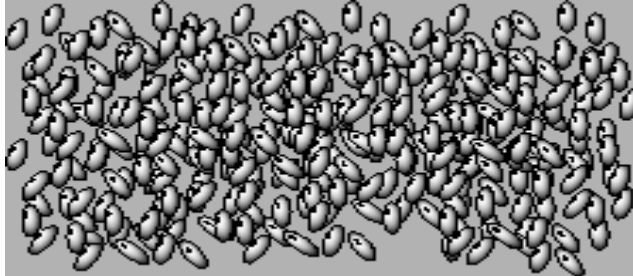


Fig 1.4 Schematic diagram of a nematic liquid crystal

The most important parameter in nematic liquid crystalline is the order parameter S , which measures how the molecules are aligned with the director \mathbf{n} . In nematic phase the molecules are able to rotate about their long axes and there are no preferential arrangements of the two ends of the molecules, hence the sign of director is of no physical significance \mathbf{n} or $-\mathbf{n}$. These kinds of molecules possess mirror symmetry and are known as Achiral Nematic Phases.

1.1.2 Chiral Nematic Liquid Crystal Phase:

Nematic phases formed by the chiral molecules i.e. no mirror symmetry, are known as chiral nematic phases. The director in cholesteric phase differs from that of the nematic phase, and varies throughout the medium in a regular way and follows a helical path. The cholesteric is characterised by the distance measured along the twist axis over which it rotate through full circle. This distance is called pitch. A cholesteric phase is nothing but a nematic phase with infinite pitch. In general there is no phase transition between the nematic and cholesteric phases in a given material, but one can form cholesteric phase from nematic phase which are doped with enantiomorphous material. The molecules forming this are optically active. The spiral arrangement of the cholesterical phase is responsible for the cholesterical colours in reflection. The reason for this to happen is the pitch of the cholesterical falls in the order of wavelength of the visible light region. The pitch of the cholesteric is very sensitive to temperature, chemical composition and applied electric or magnetic fields.

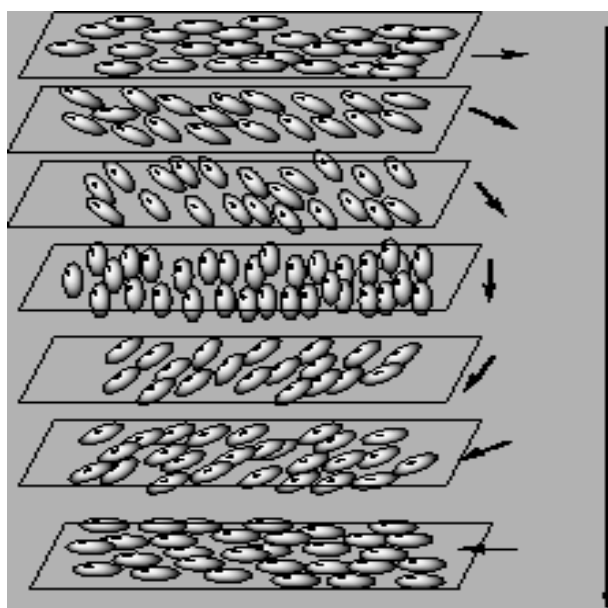


Fig.1.5 Schematic diagram of a chiral nematic liquid crystal

1.1.3 Smectic Phases:

In addition to the orientation order of the molecules some of the liquid crystals exhibit a degree of correlation in their position. This kind of liquid crystalline phases are known as smectic phases. Depending on the variation in their position they are classified into several classes. In Smectic-A, the molecules are aligned perpendicular to the layer with no long range crystalline order within a layer. These layers can slide freely over one another.

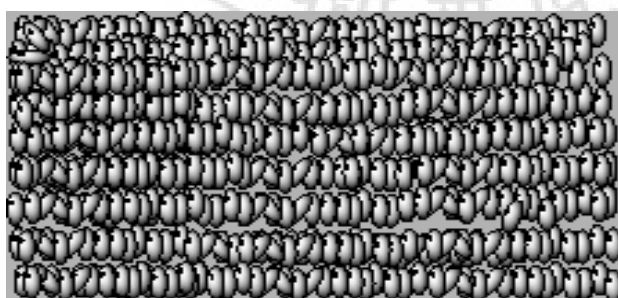


Fig.1.6 Schematic diagram of a smectic-A liquid crystal.

If the molecules are not aligned perpendicular to the layers (tilt with layers) is known as Smectic-C phase, these phases have biaxial symmetry (a phase that is also anisotropic in the

plane perpendicular to the primary director). In subsequent layers the tilt can show the same direction (syn-clinic) or it can alternate (anti-clinic).

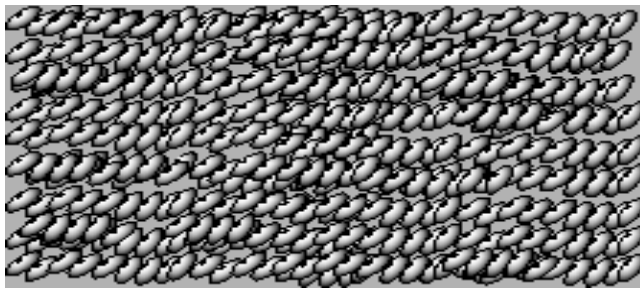


Fig.1.7 Schematic diagram of a smectic-C liquid crystal.

In Smectic-B phases, molecules possess hexagonal crystalline structure within the layers. In smectic-D one can observe the cubic structure between the layers and in Smectic-E a well ordered molecular arrangement can be found between the layers.

From the above discussion one can summarise a general transition sequence among the crystalline solids and isotropic liquids on increasing the temperature could be as follows:

Crystalline solid → Smectic Phase → Nematic phase → Isotropic phase.

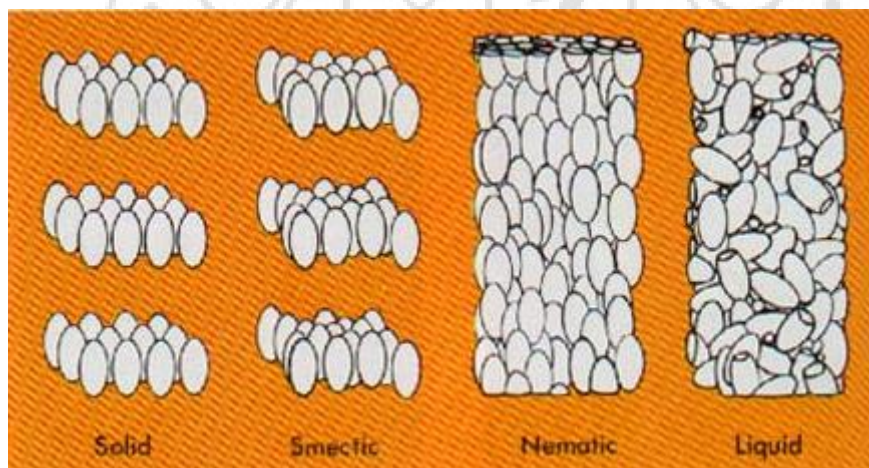


Fig.1.8 Schematic diagram matter transition on heating.

This sequence cannot be observed uniquely in all the materials. For some of the materials one or more independent phases might be absent.

1.2 Order Parameter S:

The important characteristic that differs all the liquid crystals is an orientation order of the molecules. This is the only parameter which differs the nematic and isotropic phases. For nematic phase the order parameter is non-zero ($S \neq 0$) and for isotropic phase it is zero ($S=0$).

$$S = \langle P_2(\cos\theta) \rangle = \frac{1}{2}(3 \cos^2\theta - 1)$$

Here P_2 is a second Legendre polynomial. The orientation order must be described by a second order tensor. It is not possible for the vector average of $\mathbf{n}(\mathbf{r})$ which vanishes due to liquid crystals possess a centre of symmetry. For this reason we will consider the higher order tensors. Order parameter tensor for the uniaxial liquid crystals given by de Gennes [3] in terms of diamagnetic susceptibility as:

$$Q_{ij} = x_{ij} - \frac{1}{3}\delta_{ij}x_{ij}$$

Here x_{ij} is the magnetic susceptibility tensor per unit volume; Q_{ij} is traceless the tensor of rank two.

1.3 Introduction to Flexoelectric effect in liquid crystals:

The flexoelectric effect was first found by R. B. Meyer [4], he found that geometrically asymmetric molecules or shape polarity of the molecule are responsible for a non-vanishing effect known as flexoelectric effect in mesophases. Meyer explained an example of these molecules with wedge-shaped and banana-shaped molecules. When these asymmetric molecules are brought to closer with their dipoles are pointing in up or down they will spread out or extend at their opposite direction of the dipole is called as splay. For example, wedge shaped molecules with longitudinal dipoles exhibit spontaneous polarization when they are splayed.

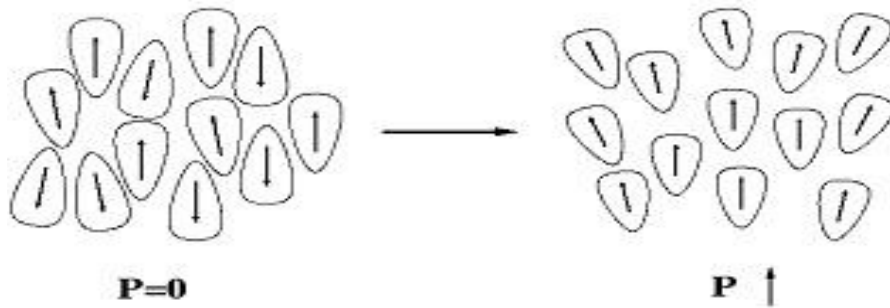


Fig.1.9 Schematic diagram of Wedge shaped molecules with longitudinal dipole.

Similarly banana shaped molecules with transverse dipoles show spontaneous polarization under bend deformation.

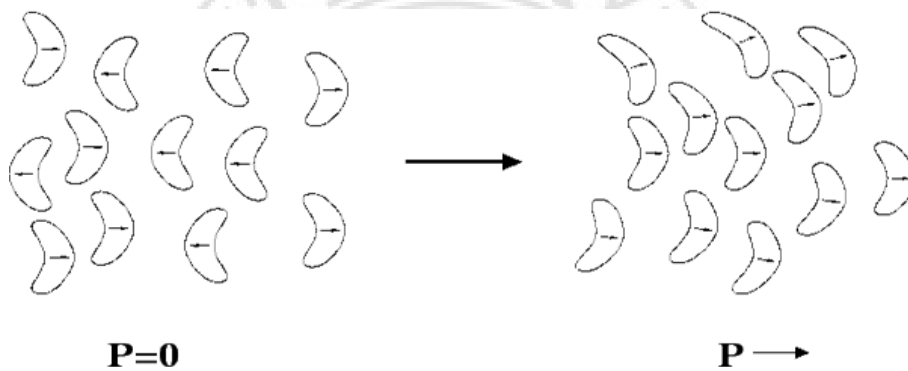


Fig.1.10 Schematic diagram of Banana shaped molecules with transverse dipole.

The asymmetric shapes of the molecules are not only the responsible for the flexoelectric effect to occur. We can also see the flexoelectric effect as a consequence of director deformation due to applied electric field induces an electrical polarization, which is analogue to the piezo-electricity effect in solid crystals. Prost and Marcerou [5] proposed a flexoelectric mechanism based on molecular quadrupoles. For quadrupolar molecules a polarization can occur due to uneven charge distributions leading to polarizations in any given volume when a splay is imposed given in fig.1.11.

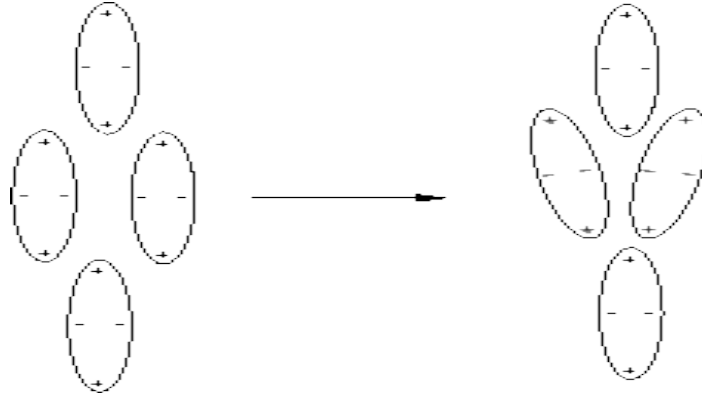


Fig.1.11 Schematic diagram of Splay deformation of a system of quadrupolar mesogens.

The motivation to study this kind of flexoelectric effect in liquid crystals which has a large influence on many phenomena in liquid crystals [6]. Technologically it plays a key role in some device applications like, flexoelectric surface switching is important in newly developed bistable displays [7, 8], flexoelectric coupling in chiral and twisted nematic crystals [9] leads to a linear rotation of the optic axis and also leads to device applications. Flexoelectric coupling in smectic liquid crystals has been shown to stabilize helical structures [10]. The flexoelectric effect is also present in lipid membranes [11].

1.3.1 Flexoelectric effect in Nematic Liquid Crystals:

In general the deformation of the molecular distribution varies from point to point within the medium. The deformations usually are described by a continuum theory where it is assumed that the magnitude of the alignment anisotropy is unchanged. The free energy due to distortion is expressed in terms of vector quantities and elastic constants k_1, k_2, k_3 . The distortion free energy density of the nematic phase is:

$$F = \frac{1}{2}(k_1(\nabla \cdot \hat{n})^2 + k_2[\hat{n} \cdot (\nabla \times \hat{n})]^2 + k_3[\hat{n} \times (\nabla \times \hat{n})]^2)$$

where k_1, k_2, k_3 are the splay, twists and bend elastic constants. For the nematic liquid crystals the spontaneous polarisation formula for the flexoelectric polarization is given by [12]

$$P = e_s \hat{n}(\nabla \cdot \hat{n}) + e_b \hat{n} \times (\nabla \times \hat{n})$$

Where the coefficients e_s and e_b are the splay and bend flexoelectric coefficients and the $\hat{n}(\nabla \cdot \hat{n})$ and $\hat{n} \times (\nabla \times \hat{n})$ are the splay and bend vectors respectively. From the above

equations one can observe the absence of twist term, because in twist there is an axis perpendicular to the helix axis which is a two-fold rotation axis any polarisation along the twist axis to be zero. Hence there is no contribution of the twist towards the polarisation of the medium. There are many experimental studies of the flexoelectric effect [13, 14]. But the measurements of coefficients e_s and e_b are difficult in order to determine from experiment, because the response of liquid crystals to applied fields is dominated by the dielectric response. For this reason the flexoelectric coefficients are not measured independently, generally $(e_s + e_b)/2$ and $(|e_s - e_b|)/2$ are measured. Besides the experimental studies, several theoretical studies have also been performed [15, 16]. An Onsager-like theory [19], a mean-field [20], and density functional theories [17, 18] have been developed. Recently more sophisticated theoretical studies have been attempted to calculate the flexoelectric coefficients using more realistic models of liquid crystals [21] and to take the effect of intermolecular interactions into account [22].

To study the splay flexoelectric effect in nematic liquid crystal with pear shape molecules we consider the Lebwohl-Lasher lattice model (LL-model) of nematic liquid crystals [23], in which at each lattice point we represent with pear-shaped molecules instead of spins at each lattice points. These pear-shaped asymmetric molecules interact with their neighbouring pear-shaped molecules giving interaction energy as given by Dhakal and Selinger [24] as:

$$H = - \sum_{\langle i,j \rangle} [A (\hat{n}_i \cdot \hat{n}_j)^2 + B (\hat{n}_i \cdot \hat{n}_j) + C \left(\frac{1 + \hat{n}_i \cdot \hat{n}_j}{2} \right)^2 \hat{r}_{ij} \cdot (\hat{n}_j - \hat{n}_i)] - \sum_i E \cdot \hat{n}_i$$

Here the first term in the Hamiltonian corresponds to the nematic order, second term corresponds to polar order and the third term represents the coupling of polar term with the splay of the nematic director. The last is the interaction with an electric field. The sum of the first three terms is taken over all pairs of nearest neighbours. There considerable interest on the relative importance of coefficients in the above equation: the coefficient A corresponds to the strong effect strong nematic ordering effect, the coefficient B corresponds to promoting a polar order and the C term gives the coupling between the nematic splay and polar order. Our project is concerned with a study of the consequences of

variation of parameters B and C in the above Hamiltonian model, looking for changes in the thermal behaviour of the system, and the resulting phase diagram.



Chapter 2:

Monte Carlo study of the flexoelectric Hamiltonian

The model Hamiltonian proposed recently was investigated with a view to examining its applicability as a function of temperature and external field [24]. As has been introduced in the last chapter, it is based on a lattice model. The study reported earlier considered this model for two combinations of the parameters influencing the polar interaction and splay coupling among the lattice sites. The thermal behaviour was simulated based on Monte Carlo methods. In this context, the objective of the present work is to explore the sub space of these few parameters to examine the relative (competing) effects of polar ordering term and the splay interaction term. We carried out simulations for different combinations of these two parameters systematically, and compose an results with those reported. This chapter thus starts with a brief introduction to Morkov chain Monte Carlo method, providing the necessary motivation and computational details. The next section presents the results of our simulations. A comparison of this work with the published data is made and new results obtained by exploring this model are included in the last section.

2.0 Need of Computer Simulation:

Computer Simulation emerged as a testing tool to find the properties of the systems in Science and Technology apart from the existing tools of Theory and Experiment. Thus we consider the Computer Simulations as 'Computer Experiments' as analogous to real Experiments because, in simulation we consider models just like materials in real laboratory experiments, and test their prediction by computing equilibrium properties under different experimental considerations using concepts equilibration statistical mechanics. In a way such simulations build bridge between the theoretical predictions and experimental observations. And inconsistencies between the two latter views can be attempted to be reconciled with simulations. If the computer simulation results are inconsistent with the theoretical approximations and consistent with the experimental results then the approximation made in theoretical study could be considered not valid. Similarly, if the computer simulation results are inconsistent with the experimental results and consistent with the theoretical approximation then the model could be incorrect. Block diagram which

shows the comparison between the theoretical prediction and experimental observation based on computer simulation is given fig.2.1

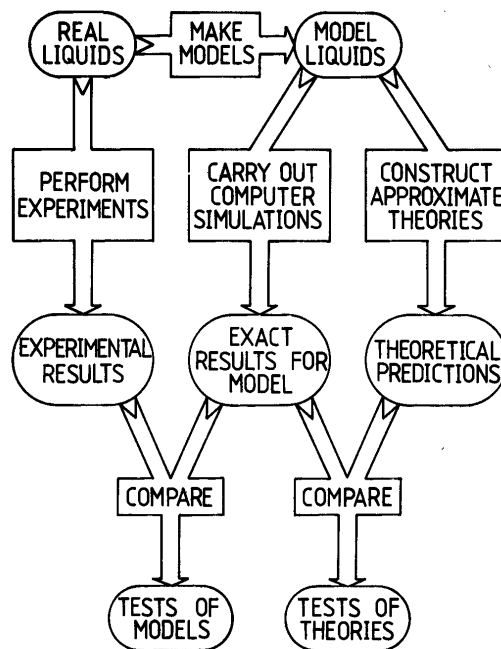


Fig.2.1 Relation between experiment, theory and computer simulation.

Computer simulations lead to reasonably accurate estimation of certain measurable macroscopic properties like, for example order parameters, their susceptibilities, energy variation with temperature, specific heat, etc., of the system. However, it should also be recognised that these simulations have their own limitations: memory of the computer, costly computer resources, statistical errors, systematic errors, etc. The statistical errors can be minimised largely by increasing the number of samples and certain systematic errors (like finite size effect) can be addressed by applying periodic boundary conditions wherever applicable. In spite of these limitations, computer simulations are more recently being recognised as a viable methodology for carrying out interest research work.

From a point of view of statistical mechanics of model systems, computer simulations are broadly divided into Molecular Dynamics Simulation and Monte Carlo Simulation. Molecular Dynamics method is used to study the time averaged properties of the system by (approximately) solving the equations of motion which describes the time evolution. Monte Carlo method gives the ensemble averaged properties of the system using a stochastic algorithm. In the present context we used Monte Carlo Simulation.

2.1 Monte Carlo Simulation:

Morkov Chain Monte Carlo method [25] asserts that for a desired probability distribution in some (configuration) space, provided that space is ergodic, one can construct an appropriate transition matrix which specifies the probability of jumping from an initial state to a next state. Looking for a convenient algorithm to help construct this matrix is an important step to proceed further. The celebrated Metropolis algorithm is extensively used for this purpose and we present briefly the details in the next section. An important requirement of this algorithm is the ability to propose a random step in the configuration space before its acceptability criteria could be determined. It should not perhaps come as a surprise, but strictly it is just not possible. There could only be pseudo-random sequences which can perhaps be appropriated to true random sequences to a reasonable simulations are good random number generators. An illustrative use of such a sequence in a simple experiment like determination of the value of π is given in fig.2.2. It is obvious that more random the distribution of point in the plane is, the better will be the estimate.

In real physical systems in equilibrium we do not have the corresponding microstates distributed uniformly like fig.2.2, but according to a statistical law, like Maxwell-Boltzmann distribution. One has a problem of constructing an ensemble of microstates which is equilibrated at the desired temperature T , and has the probability distribution function (PDF) given by:

$$P(E) \propto e^{-\beta E}$$

where $\beta = \frac{1}{K_{\beta}T}$. We now present an algorithm which helps the system to take a series of transitions according to a prescribed set of probabilities, given that the system is finally guided to the neighbourhood of the ensemble, no matter what this initial state is. The system thereafter evolves through this prescription such that it samples the configuration space according to the above prescription.

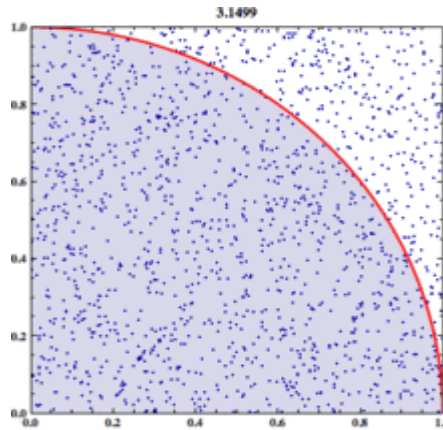


Fig.2.2 Monte Carlo method applied to approximating the value of π .

2.2 Metropolis Algorithm:

Metropolis Algorithm provides a chain of microstates known as Markov chain. Consider a chain of microstates with initial state C_0 ,

$$C_0 \rightarrow C_1 \rightarrow C_2 \rightarrow \dots \rightarrow C_K \rightarrow C_{K+1} \rightarrow \dots$$

For illustrative purpose, consider that all microstates are visited by assigning a set of random variables (say, spin) a value of +1 or -1 and all the microstates are equally probable. Let us select one of the states C_i whose spin is S_i at lattice site i and calculate the energy of this configuration (C_i). Now flip the spin of this state from spin $S_i \rightarrow -S_i$ and calculate its energy as $E(C_t)$ a trial microstate C_t . Accept the trial microstate as next microstate in Markov chain with a probability given by:

$$P = \min \left(1, \frac{\pi(C_t)}{\pi(C_i)} \right)$$

$$= \min(1, e^{-\beta \Delta E}) \quad \text{where } \Delta E = E(C_t) - E(C_i)$$

Or in other words:

$$C_{i+i} = C_t \quad \text{with probability } P$$

$$= C_i \quad \text{with probability } 1-P$$

This completes the acceptance or rejection of the trial microstate C_t , which defines the transition matrix ω . This completes one Monte Carlo Step (MCS). We do the same procedure for the total N lattice points in the system (so as to span all degrees of freedom) which gives one Monte Carlo Sweep. Repeat this process for large number of times so that the algorithm produces a Markov chain with the final invariant probability distribution as the desired function. This can be summarized as follows:

- Pick a state randomly as an initial microstate C_k of a lattice site i , calculate its energy as $E(C_i)$ whose spin is S_i , now flip the spin of the randomly selected state from $S_i \rightarrow -S_i$ and calculate its energy by considering as trial configuration C_t as $E(C_t)$.
- If $\Delta E = E(C_t) - E(C_i) \leq 0$, then accept the trial state: $C_{k+1} = C_t$.
- If $\Delta E = E(C_t) - E(C_i) > 0$, then generate a random number ζ in interval $[0,1]$.
 - If $\zeta \leq e^{-\beta\Delta E}$, then accept the trial state: $C_{k+1} = C_t$.
 - If $\zeta > e^{-\beta\Delta E}$, then reject the trial state: $C_{k+1} = C_k$.
- Iterate this for large number of times.

The transition matrix what we get should be consistent with the detailed balance condition:

$$\omega_{i \leftarrow j} \pi_j = \omega_{j \leftarrow i} \pi_i$$

Where π 's are the probabilities of the state and ω is the transition probabilities from one state i , say, to another j . The acceptance probability $p(x)$ given by Metropolis is not continuous at $x=0$. Glauber [26] proposed the probability which is agreement with the detailed balance condition as:

$$P(x) = \frac{1}{1+e^x}$$

This is shown in fig.2.3. The solid line represents the Metropolis acceptance probability $P(x)$ and dashed line represents the probability $P(x)$ proposed by Glaber.

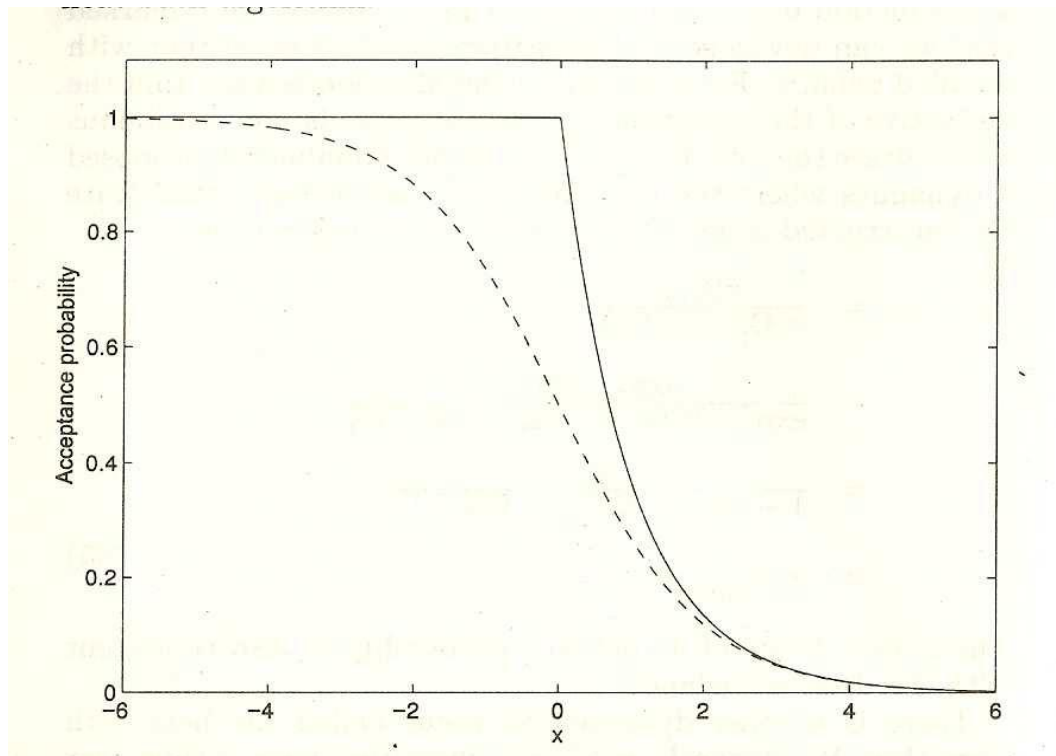


Fig.2.3 Acceptance probability, $p(x)$ with change in energy. The solid line refers to the Metropolis sampling and dashed line refers the Glauber dynamics.

2.3 Physical Systems:

The physical systems one can study using Computer simulations are classified broadly into two types based on the translational property. They are off-lattice model: in which the molecules have both positional and orientation degree of freedom. In lattice model the molecules have orientation degree of freedom order only, and they do not have translation in space. Liquid crystal phase transition of Isotropic to Nematic depends only on the orientation degree of freedom; hence it is convenient to use the lattice models to study the physical properties of the liquid crystals. In these lattice models we represent each lattice site with a unit vector corresponding to the molecular orientation in three dimensions. The simple model we used to study the liquid crystals is Lebwohl-Lasher lattice model (LL-model) [27]. We minimise the finite size effects, if we considering a bulk material by introducing periodic boundary conditions. Fig.2.4 shows the scheme of periodic boundary conditions in two dimensional systems.

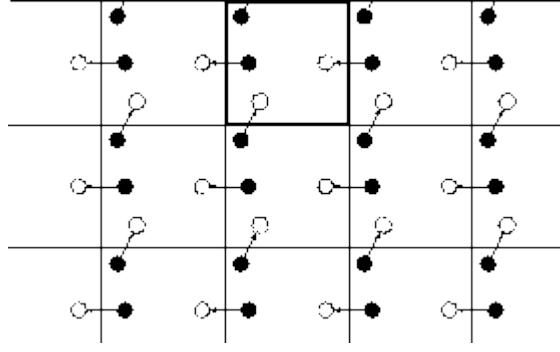


Fig.2.4 Periodic boundary conditions the central box is outlined by a thicker line.

2.4 Effect of parameters used in the Hamiltonian:

The Hamiltonian proposed by Dhakal [4] in his recent work consists of four terms :

$$H = - \sum_{\langle i,j \rangle} [A (\hat{n}_i \cdot \hat{n}_j)^2 + B (\hat{n}_i \cdot \hat{n}_j) + C \left(\frac{1 + \hat{n}_i \cdot \hat{n}_j}{2} \right)^2 \hat{r}_{ij} \cdot (\hat{n}_j - \hat{n}_i)] - \sum_i E \cdot \hat{n}_i \quad (1)$$

Here the first term $-A(\hat{n}_i \cdot \hat{n}_j)^2$ corresponds to the nematic ordering terms of LL-model, second term $-B (\hat{n}_i \cdot \hat{n}_j)$ corresponds to polar ordering mechanism as in the Heisenberg model of magnetism and the third term $-C \left(\frac{1 + \hat{n}_i \cdot \hat{n}_j}{2} \right)^2 \hat{r}_{ij} \cdot (\hat{n}_j - \hat{n}_i)$ represents the coupling of polar term with the splay of the nematic director. The last is the coupling to the external field. The sum of the first three terms is taken over the pairwise interaction of all the nearest neighbours. There is very much curiosity about the coefficients in the above equation, the coefficient A corresponds to the strong effect to induce polar nematic uniaxial order, the coefficient B promotes polar order and thereby breaking \hat{n} to $-\hat{n}$ symmetry, and C term introduces a coupling between the nematic splay and the polar order. We first review the earlier simulation work [24]: A system of pear-like molecules interacting with the lattice Hamiltonian of Eq. (1) on a 20x20x20 cubic lattice system is considered. Periodic boundary conditions along Z-axis, and free boundary conditions along the X-axis and Y-axis were implemented, so as to allow formation of splay distribution in the X-Y plane. Metropolis algorithm was used to simulate equilibrium ensembles, and various averages of physical properties are computed. The parameters of interest are:

$$\text{Order parameter: } \langle S \rangle = \frac{1}{N} \sum_{\langle ij \rangle} (1.5 \cos^2 \theta - 0.5).$$

$$\text{Polar Order} \quad : \quad \langle P \rangle = \frac{1}{N} \sum_{\langle i \rangle} \hat{d} \cdot \hat{n}_i$$

Splay Vector :

$$\langle \theta \rangle = [\hat{n}(\nabla, \hat{n})]_{i,j} = \frac{1}{2} [\hat{n}_j(\hat{r}_{ij} \cdot \hat{n}_j) - \hat{n}_i(\hat{r}_{ij} \cdot \hat{n}_i) + \hat{n}_i(\hat{n}_i \cdot \hat{n}_j)(\hat{r}_{ij} \cdot \hat{n}_j) - \hat{n}_j(\hat{n}_i \cdot \hat{n}_j)(\hat{r}_{ij} \cdot \hat{n}_i)]$$

Here $\alpha, \beta = x, y, z$ and N is the total number of lattice sites. The eigenvector corresponding to the largest eigenvalue of the nematic order tensor $Q_{\alpha\beta}$ is the instantaneous director \hat{d} . The splay vector calculated from the above equation is averaged over the four bonds in the (x, y) plane. The magnitude of this vector gives the average angle between the molecular orientations on neighbouring lattice sites $\langle \theta \rangle$. The last composition takes significant computational time since for every microstate the eigenvector corresponding to its director has to be computed to be calculating this in quantity. In this respect, it differs from the computational simplicity of the LL-model, and limits the size of the system, for a given set of limitation on the time available for such computations. We show the typical results reported earlier [24], for specific choice of the parameters as given in the figure caption (fig.2.5). These computations were carried out without a field, and hence represent the thermal evolution of the system under different condition of competing polar and splay ordering terms.

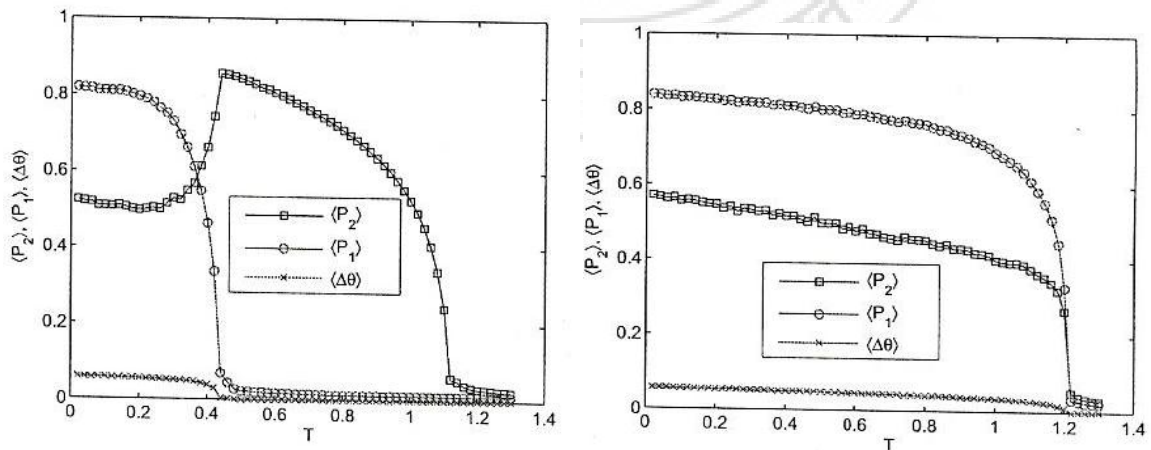


Fig.2.5 Monte Carlo simulation results for the order parameters (a) $\langle S \rangle$, $\langle P \rangle$ and $\langle \theta \rangle$ for $A=1.5$, $B=0.09$ and $C=0.3$ (b) $\langle S \rangle$, $\langle P \rangle$ and $\langle \theta \rangle$ for $A=1.5$, $B=0.4$ and $C=0.3$ as functions of temperature T .

The observations are as follows: the above plots show the variation of order parameter, polar parameter and splay order with the temperature for various value of A, B and C. In plot (a) the values for the coefficient taken as $A = 1.5$, $B = 0.09$ and $C = 0.3$ with zero applied electric field, with this set it is observed that the Isotropic-nematic transition takes place at a high temperature, the nematic order parameter develops from zero to a non-zero value around $T=1.1$ and the polar and splay order are zero across this transition. At low temperature ($T \sim 0.4$) the polar order suddenly increases from zero accompanied by the splay order leading to a non-zero value. During this process the nematic order decreases and settles at a value lower than the polar order. The splay order saturates at about 0.06. By increasing the value of B from 0.09 to 0.4 while keeping A and C fixed as above, a direct transition from Isotropic to polar order has been reported as shown in fig.2.5, nematic, polar, as well as the splay orders all changing from their high temperature zero value across the transition. These results are illustrated in fig2.6.

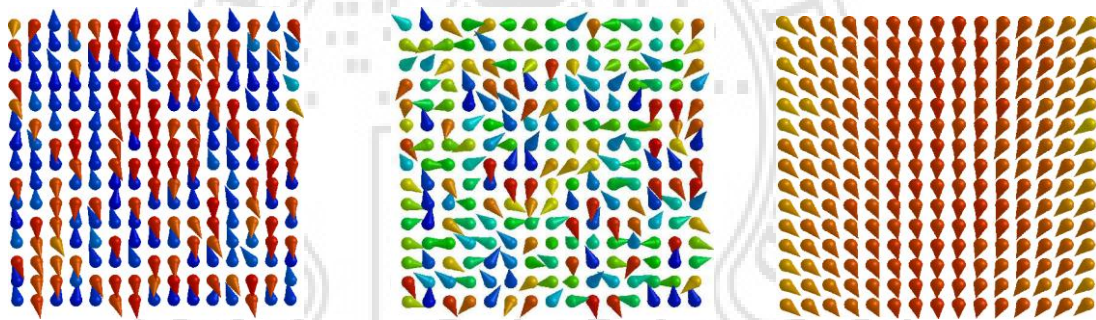


Fig.2.6 Simulation results in the three phases: (a) Isotropic. (b)Nematic(c) Polar

The present work is motivated by earlier results. The curiosity was in the evolution of the first phase diagram in fig.2.5 to the second as a simple parameter B is varied from 0.09 to 0.4 with systematically over a range of values of B and C, with no external field. While the details of these computations are reserved for a discussion later, we wish to point out that our prediction based on this Hamiltonian differ qualitatively from this work, and even for the choice indicated in fig.2.5, our simulations indicates the outcome very differently.

To proceed further, we first present some details of the Monte Carlo simulations carried out. Because of the large number of computation involved we restricted the size of the system to $10 \times 10 \times 10$. We applied periodic boundary conditions in the Z-direction, while leaving the free-boundary conditions in the X-Y plane. We find that 10^5 runs are adequate

for equilibration for this small system, and the production run comprises of another 10^5 lattice sweeps. The temperature is varied from 0.04 to 2 in steps of 0.04 (all in reduced limits of the LL interaction strength contained in the first term of the Hamiltonian Eq. (1)). We varied B from 0.1 to 0.9 in steps of 0.2, and similarly C has been varied for each of these B values again from 0.1 to 0.9 in steps of 0.2. Thus we have in total 25 sets of [B, C] pairs. We further supplement this subspace of (B, C) parameters with certain choice values: (0.4, 0), (0.4, 0.3), (0.4, 0.5); (0.6, 0.3), (0.6, 0.5) as an after thought on examining the initial set. The data presented in this dissertation thus report on the thermal evolution of the system, transition from a high temperature isotropic state to a low temperature nematic (and polar) state, at these 30 pairs of values of (B, C). The computed thermal averages in each case include the orientational order parameter S, the polar order parameter P, the splay order parameter θ , the specific heat (at constant volume) C_V , the variance in the equilibrium fluctuations in S (χ_S), and those in P (χ_P). Thus at each set (B, C), we have six plots indicating the physical behaviour of the system with respect to temperature T. to make the presentation less cluttered, we presented in Table-1 a guide to the figures presented in this respect depicting the various results encompassing all the possibilities mentioned above. The individual figure captions of course provide description separately. These figures show evidences of different transition as peaks in C_V , χ_S and χ_P as the case may be. in certain cases, there are no such sharp features, but unmistakable broad variations are observed. Such of those descriptive observations are summarized in Table-2. Finally certain qualitative data on the location of the transition temperatures, etc., are provided in Table-3, for easy reference. The discussion presented in the next section refers to these Tables.

Table-1: Results graphs

A=1.5	B=0.1	C	Plots between	Plot No.		
		0.1	Orientation order S v/s	Fig.2.7		
		0.3	Temperature			
		0.5	Polar order P v/s	Fig.2.8		
		0.7	Temperature			
		0.9	Splay orientation θ v/s	Fig.2.9		
			Temperature			
			Specific heat C_V v/s	Fig.2.10		
			Temperature			
			Fluctuations in S (χ_S)	Fig.2.11		
			v/s Temperature			
			Fluctuations in P (χ_P)	Fig.2.12		
			v/s Temperature			
		A=1.5	B=0.3	C=0.1	Orientation order S v/s	Fig.2.13
				0.3	Temperature	
				0.5	Polar order P v/s	Fig.2.14
				0.7	Temperature	
		0.9	Splay orientation θ v/s	Fig.2.15		
			Temperature			
			Specific heat C_V v/s	Fig.2.16		
			Temperature			
			Fluctuations in S (χ_S)	Fig.2.17		
			v/s Temperature			
			Fluctuations in P (χ_P)	Fig.2.18		
			v/s Temperature			
A=1.5	B=0.5	C=0.1	Orientation order S v/s	Fig.2.19		
		0.3	Temperature			
		0.5	Polar order P v/s	Fig.2.20		
		0.7	Temperature			

		0.9	Splay orientation θ v/s Temperature	Fig.2.21
			Specific heat C_V v/s Temperature	Fig.2.22
			Fluctuations in $S(\chi_S)$ v/s Temperature	Fig.2.23
			Fluctuations in $P(\chi_P)$ v/s Temperature	Fig.2.24
A=1.5	B=0.7	C= 0.1	Orientation order S v/s Temperature	Fig.2.25
		0.3		
		0.5	Polar order P v/s Temperature	Fig.2.26
		0.7		
		0.9	Splay orientation θ v/s Temperature	Fig.2.27
			Specific heat C_V v/s Temperature	Fig.2.28
			Fluctuations in $S(\chi_S)$ v/s Temperature	Fig.2.29
			Fluctuations in $P(\chi_P)$ v/s Temperature	Fig.2.30
A=1.5	B=0.9	0.1	Orientation order S v/s Temperature	Fig.2.31
		0.3		
		0.5	Polar order P v/s Temperature	Fig.2.32
		0.7		
		0.9	Splay orientation v/s Temperature	Fig.2.33
			Specific heat C_V v/s Temperature	Fig.2.34
			Fluctuations in $S(\chi_S)$ v/s Temperature	Fig.2.35
			Fluctuations in $P(\chi_P)$	Fig.2.36

			v/s Temperature	
A=1.5	B=0.4	0.0	Orientation order S v/s	Fig.2.37
		0.3	Temperature	
		0.5	Polar order P v/s	Fig.2.38
			Temperature	
			Splay orientation θ v/s	Fig.2.39
			Temperature	
			Specific heat C_V v/s	Fig.2.40
Temperature				
Fluctuations in S (χ_S)	Fig.2.41			
v/s Temperature				
Fluctuations in P (χ_P)	Fig.2.42			
v/s Temperature				
A=1.5	B=0.6	0.3	Orientation order S v/s	Fig.2.43
		0.5	Temperature	
		0.5	Polar order P v/s	Fig.2.44
			Temperature	
			Splay orientation θ v/s	Fig.2.45
			Temperature	
			Specific heat C_V v/s	Fig.2.46
Temperature				
Fluctuations in S (χ_S)	Fig.2.47			
v/s Temperature				
Fluctuations in P (χ_P)	Fig.2.48			
v/s Temperature				

Table-2: T_s = Transition temperature of orientation

T_p = Transition temperature of polar order

A=1.5 B=0.1	C	Temperature			
		Order parameters	Fluctuations		
			C_V	χ_S	χ_P
0.1	$T_s = 1.0$ $T_p = 0.28$	0.28,0.4,1.0	0.28,1.0	0.28	
0.3	$T_s = 1.0$ $T_p = 0.36$	0.36,1.0	0.36,1.0	0.36	
0.5	$T_s = 0.40,1.0$ $T_p = 0.36$	0.36,1.0	0.44,1.0	0.36,0.6,-	
0.7	$T_s = 0.40,1.0$ $T_p = 0.32$	0.32,0.40,1.0	0.4,1.0	0.28	
0.9	$T_s = -$ $T_p = -$	0.04,0.20,0.28,1.0	0.04,0.20,0.28,1.0	0.04,0.20,0.28,-	
A=1.5 B=0.3	C				
0.1	$T_s = 0.52,1.0$ $T_p = 0.56$	0.56,1.0	0.52,1.0	0.56	
0.3	$T_s = -,1.04$ $T_p = -, 0.72$	0.52,0.72,1.04	0.52,1.04	0.56,0.72	
0.5	$T_s = -,1.04$	0.44,0.76,1.04	0.48,1.04	0.52,-	

		$T_p = -,0.76$			
	0.7	$T_s = -,1.04$ $T_p = -,0.76$	0.44,0.76,1.04	0.48,1.04	0.52,-
	0.9	$T_s =$ 0.32,1.04 $T_p =$ 0.32,0.76	0.28,0.36,0.68,0.80,0.88,1.04	0.28,0.36,0.80,0.88,1.04	0.28,0.40,-
A=1.5 B=0.5	C				
	0.1	$T_s = 1.2$ $T_p = -$	0.56,1.24	0.56,1.24	0.64,-
	0.3	$T_s =$ 0.48,1.2 $T_p =$ 0.40,0.80	0.48,0.84,1.24	0.52,1.2	0.6,-
	0.5	$T_s =$ 0.44,1.2 $T_p = 0.48,-$	0.48,1.2	0.48, 1.24	0.52,-
	0.7	$T_s =$ 0.52,1.2 $T_p = 0.52,-$	0.52,1.2	0.52,1.2	0.52,-
	0.9	$T_s =$ 0.44,1.20 $T_p =$ 0.44,0.52	0.44,1.20	0.44,1.20	0.44,0.52,-
A=1.5 B=0.7	C				
	0.1	$T_s =$ 0.56,1.44	0.56,1.44	0.6,1.44	0.64,-

		$T_p = 0.56,-$			
	0.3	$T_s =$ 0.56,1.44 $T_p = 0.56,-$	0.56,1.44	0.36,0.56,1.44	0.36,0.68,-
	0.5	$T_s =$ 0.52,1.44 $T_p = 0.52,-$	0.52,1.44	0.52,1.44	0.56,-
	0.7	$T_s =$ 0.56,1.44 $T_p = 0.56,-$	0.44,0.56,1.44	0.56,1.44	0.56,-
	0.9	$T_s =$ 0.40,1.40 $T_p =$ 0.40,0.52	0.40,1.40	0.44,1.40	0.56,-
A=1.5 B=0.9	C				
	0.1	$T_s =$ 0.60,1.68 $T_p = 0.60,-$	0.6,1.68	0.64,1.68	0.72,-
	0.3	$T_s =$ 0.64,1.68 $T_p = 0.64,-$	0.52,1.68	0.64,1.68	0.64,-
	0.5	$T_s =$ 0.60,1.68 $T_p = 0.60$	0.56,1.68	0.56,1.68	0.6,-
	0.7	$T_s =$ 0.60,1.68 $T_p = 0.60,-$	0.52,1.68	0.52,1.68	0.6,-
	0.9	$T_s =$ 0.44,1.68	0.36,0.44,0.52,1.68	0.36,0.44,0.52,1.68	0.36,0.44,0.5 2,-

		$T_p = 0.44,-$			
A=1.5 B=0.4	C				
	0.0	$T_s = 1.12$ $T_p = 0.28$	1.12	1.12	0.40,-
	0.3	$T_s = 1.12$ $T_p = 0.8$	0.48,0.8,1.12	0.52,1.12	0.52,-
	0.5	$T_s = 1.12$ $T_p = 0.84$	0.52, 0.84,1.12	0.52,1.12	0.52,-
A=1.5 B=0.6	C				
	0.3	$T_s = 1.28$ $T_p = -$	0.52,1.32	0.52,1.32	0.6,-
	0.5	$T_s = 1.32$ $T_p = -$	0.36,0.52,1.32	0.36,0.52,1.32	0.36,0.6,-

(- indicates no specific transition).

Table-3: Observations.

A=1.5, B=0.1	C	Order parameter v/s Temperature	Specific heat v/s Temperature	Fluctuations v/s Temperature		Remarks
				Fluctuations In S (χ_s)	Fluctuations In P (χ_P)	
	0.1	T_c of S is near 1.0 T_c of P is near 0.28	Observed peaks at 0.24,0.40,1.0	χ_s gives peaks at T_c of both S and P	χ_P gives peaks at T_c of P= 0.28	Fluctuations in χ_s near T_c of P
	0.3	T_c of S is near 1.0 T_c of P is near 0.36	Observed peaks at 0.36,1.0	χ_s gives peaks at T_c of both S and P	χ_P gives peaks at T_c of P=0.36	Small fluctuations in χ_s near T_c of P
	0.5	T_c of S is near 1.1 T_c of P is near 0.4	Observed peaks at 0.36,1.0	χ_s gives peaks at T_c of both S and P, no sharp decrease of χ_P after T_c of P	χ_P gives peaks at T_c of P=0.36,0.6, a fter that no sharp decrease χ_P	Large fluctuations in χ_P after T_c of P
	0.7	T_c of S is near 1.1 T_c of P is near 0.4	Observed peaks at 0.32,0.40,1.0	χ_s gives peaks at T_c of both S and P	χ_P gives peaks at T_c of P=0.28	Small fluctuations in χ_s near T_c of P
	0.9	no specific transition in both S and P	Observed peaks at 0.04,0.20,0.28,1 .0	χ_s gives peaks at 0.04,0.20,0.2 8,1.0	χ_P gives peaks at 0.04,0.20,0.2 8, after that	Fluctuations in χ_s and χ_P are similar

					no sharp decrease χ_P	
A=1.5, B=0.3	0.1	T_c of S is near 0.52,1.0 T_c of P is near 0.56	Observed peaks at 0.56,1.0	χ_S gives peaks at T_c of both S and P	χ_P gives peaks at T_c of P= 0.56	Fluctuations in χ_S near T_c of P
	0.3	T_c of S is near 1.04 T_c of P is near 0.72	Observed peaks at 0.52,0.72,1.04	χ_S gives peaks at T_c of both S and P	χ_P gives peaks at T_c of P=0.52,0.72	Small fluctuations in χ_S near T_c of P
	0.5	T_c of S is near 1.04 T_c of P is near 0.76	Observed peaks at 0.44,0.76,1.04	χ_S gives peaks at T_c of both S and P, no sharp decrease of χ_P after T_c of P	χ_P gives peaks at T_c of P=0.52, after that no sharp decrease χ_P	Large fluctuations in χ_P after T_c of P
	0.7	T_c of S is near 1.04 T_c of P is near 0.76	Observed peaks at 0.44,0.76,1.04	χ_S gives peaks at T_c of both S and P	χ_P gives peaks at T_c of P=0.52, after that no sharp decrease χ_P	Small fluctuations in χ_S near T_c of P
	0.9	T_c of S is near 0.32,1.04 T_c of P is near 0.32,0.76	Observed peaks at 0.28,0.36,0.68,0.80,0.88,1.04	χ_S gives peaks at 0.28,0.36,0.68,0.80,0.88,1.04	χ_P gives peaks at 0.28,0.40, after that no sharp decrease χ_P	Large fluctuations at low temperature in both χ_S and χ_P

A=1.5, B=0.5	0.1	T_c of S is near 1.20, no specific transition in P	Observed peaks at 0.56,1.24	χ_s gives peaks at T_c of both S and P	χ_P gives peaks at T_c of P= 0.64, after that no sharp decrease χ_P	Fluctuations in χ_s near T_c of P
	0.3	T_c of S is near 0.48,1.20 T_c of P is near 0.40,0.80	Observed peaks at 0.48,0.84,1.24	χ_s gives peaks at T_c of both S and P	χ_P gives peaks at T_c of P=0.64,	Small fluctuations in χ_s near T_c of P
	0.5	T_c of S is near 0.44,1.20 T_c of P is near 0.48	Observed peaks at 0.48,1.20	χ_s gives peaks at T_c of both S and P, no sharp decrease of χ_P after T_c of P	χ_P gives peaks at T_c of P=0.52, after that no sharp decrease χ_P	Large fluctuations in χ_P after T_c of P
	0.7	T_c of S is near 0.52,1.20 T_c of P is near 0.76	Observed peaks at 0.52,1.20	χ_s gives peaks at T_c of both S and P	χ_P gives peaks at T_c of P=0.52, after that no sharp decrease χ_P	Small fluctuations in χ_s near T_c of P
	0.9	T_c of S is near 0.44,1.20 T_c of P is near 0.44,0.52	Observed peaks at 0.44,1.20	χ_s gives peaks at T_c of both S and P	χ_P gives peaks at 0.44,0.52, after that no sharp decrease χ_P	Large fluctuations at low temperature in both χ_s and χ_P

A=1.5, B=0.7	0.1	T_c of S is near 0.56,1.44 T_c of P is near 0.56	Observed peaks at 0.56,1.44	χ_s gives peaks at T_c of both S and P	χ_P gives peaks at T_c of P= 0.64, after that no sharp decrease χ_P	Fluctuations in χ_s near T_c of P
	0.3	T_c of S is near 0.56,1.44 T_c of P is near 0.56	Observed peaks at 0.56,1.44	χ_s gives peaks at T_c of both S and P	χ_P gives peaks at 0.36,0.68, after that no sharp decrease χ_P	Small fluctuations in χ_s near T_c of P
	0.5	T_c of S is near 0.52,1.44 T_c of P is near 0.52	Observed peaks at ... 0.44,0.56,1.44	χ_s gives peaks at T_c of both S and P, no sharp decrease of χ_P after T_c of P	χ_P gives peaks at T_c of P=0.56, after that no sharp decrease χ_P	Large fluctuations in χ_P after T_c of P
	0.7	T_c of S is near 0.56,1.44 T_c of P is near 0.56	Observed peaks at 0.44,0.56,1.44	χ_s gives peaks at T_c of both S and P	χ_P gives peaks at T_c of P=0.56, after that no sharp decrease χ_P	Small fluctuations in χ_s near T_c of P
	0.9	T_c of S is near 0.40,1.40 T_c of P is near 0.40,0.52	Observed peaks at 0.40,1.40	χ_s gives peaks at T_c of both S and P	χ_P gives peaks at T_c of P=0.56, after that no	Large fluctuations at low temperatur

					sharp decrease χ_P	e in both χ_S and χ_P
A=1.5, B=0.9	0.1	T_c of S is near 0.60,1.68 T_c of P is near 0.60	Observed peaks at 0.60,1.68	χ_S gives peaks at T_c of both S and P	χ_P gives peaks at T_c of P= 0.72, after that no sharp decrease χ_P	Fluctuations in χ_S near T_c of P
	0.3	T_c of S is near 0.64,1.68 T_c of P is near 0.56	Observed peaks at 0.52,1.68	χ_S gives peaks at T_c of both S and P	χ_P gives peaks at 0.64, after that no sharp decrease χ_P	Small fluctuations in χ_S near T_c of P
	0.5	T_c of S is near 0.60,1.68 T_c of P is near 0.60	Observed peaks at 0.56,1.68	χ_S gives peaks at T_c of both S and P, no sharp decrease of χ_P after T_c of P	χ_P gives peaks at T_c of P=0.60, after that no sharp decrease χ_P	Large fluctuations in χ_P after T_c of P
	0.7	T_c of S is near 0.60,1.68 T_c of P is near 0.60	Observed peaks at 0.52,1.68	χ_S gives peaks at T_c of both S and P	χ_P gives peaks at T_c of P=0.60, after that no sharp decrease χ_P	Small fluctuations in χ_S near T_c of P
	0.9	T_c of S is near 0.44,1.68	Observed peaks at	χ_S gives peaks at	χ_P gives peaks at T_c of	Large fluctuations

		T_c of P is near 0.60	0.36,0.44,0.52,1.68	0.36,0.44,0.52,1.68	P=0.36,0.44,0.52, after that no sharp decrease χ_P	at low temperature in both χ_S and χ_P
A=1.5, B=0.4	0.0	T_c of S is near 1.12 and a dip at T_c of P, T_c of P is near 0.28	Peak at 1.12	Peak at 1.12	χ_P gives peak at 0.40, after that no sharp decrease χ_P	no fluctuations in χ_S near T_c of P
	0.3	T_c of S is near 1.12 and a dip at T_c of P, T_c of P is near 0.8	Peaks at 0.48,0.80,1.12	Peaks at 0.52,1.12	χ_P gives peak at 0.52, after that no sharp decrease χ_P	Large fluctuations at low temperature in both χ_S and χ_P
	0.5	T_c of S is near 1.12 and a dip at T_c of P, T_c of P is near 0.84	Peaks at 0.52,0.84,1.12	Peaks at 0.52,1.12	χ_P gives peak at 0.52, after that no sharp decrease χ_P	Large fluctuations at low temperature in both χ_S and χ_P
A=1.5, B=0.6	0.3	T_c of S is near 1.28 and a dip at T_c of P, no specific transition in P	Peaks at 0.52,1.32	Peaks at 0.52,1.32	χ_P gives peak at 0.60, after that no sharp decrease χ_P	Large fluctuations at low temperature in both χ_S and χ_P
	0.5	T_c of S is near	Peaks at	Peaks at	χ_P gives	Large

		1.32 and a dip at T_c of P, no specific transition in P	0.36,0.52,1.32	0.36,0.52,1.32 2	peak at 0.6, after that no sharp decrease χ_P	fluctuations at low temperature in both χ_S and χ_P



Plots:

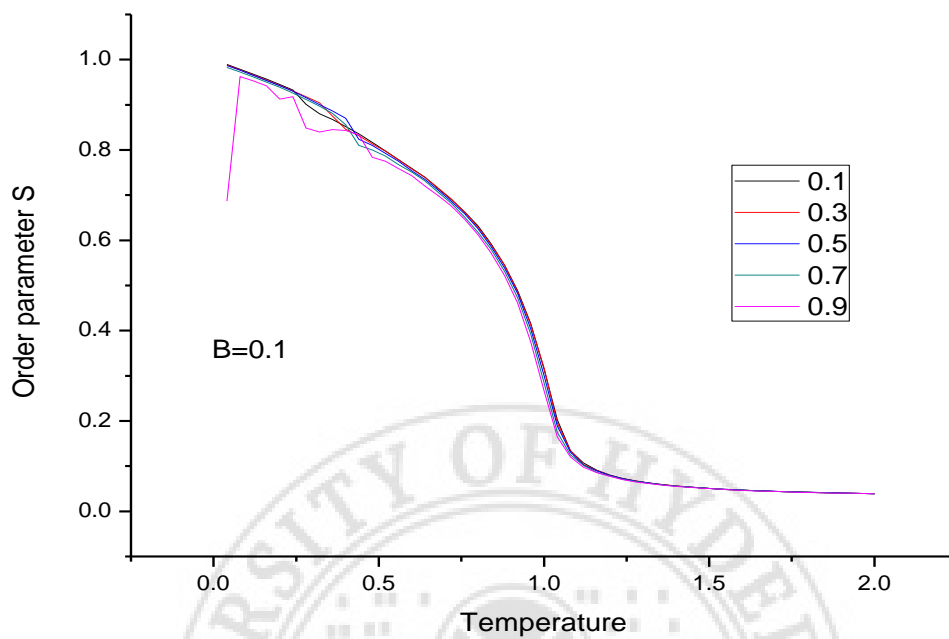


Fig.2.7 Order parameter S v/s Temperature for various values of C

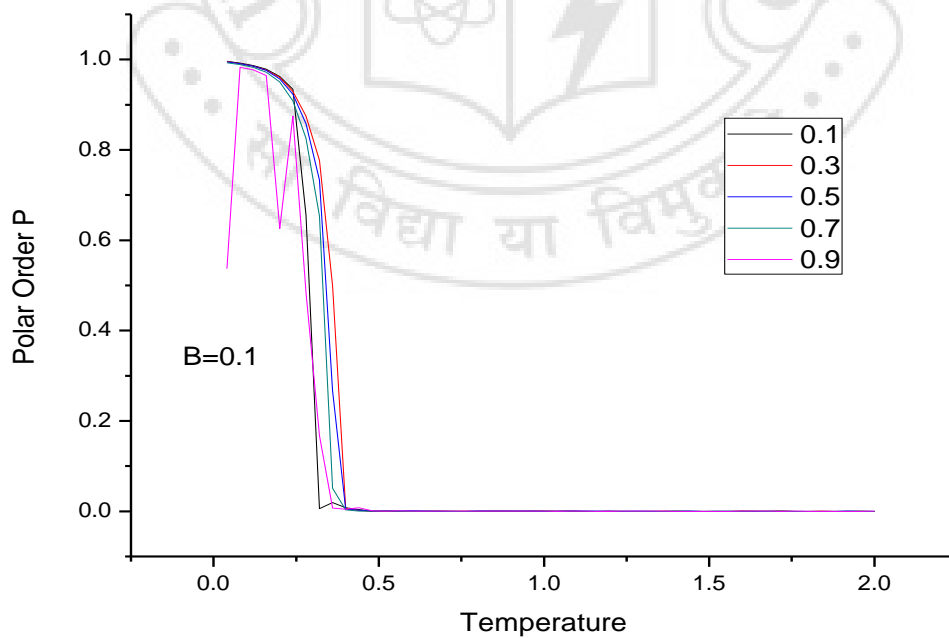


Fig.2.8 Polar order P v/s Temperature for various values of C

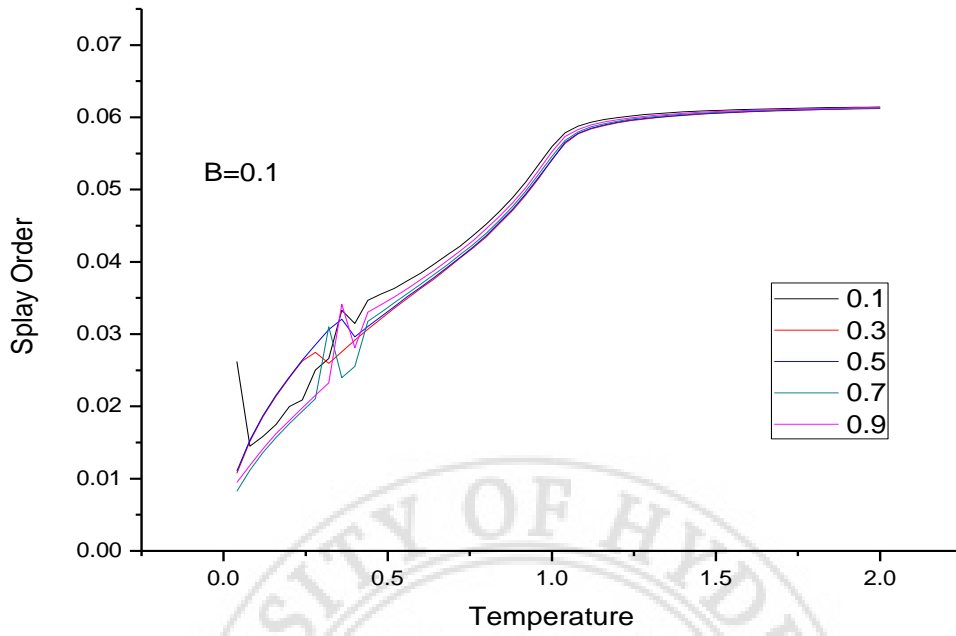


Fig.2.9 Splay order θ v/s Temperature for various values of C

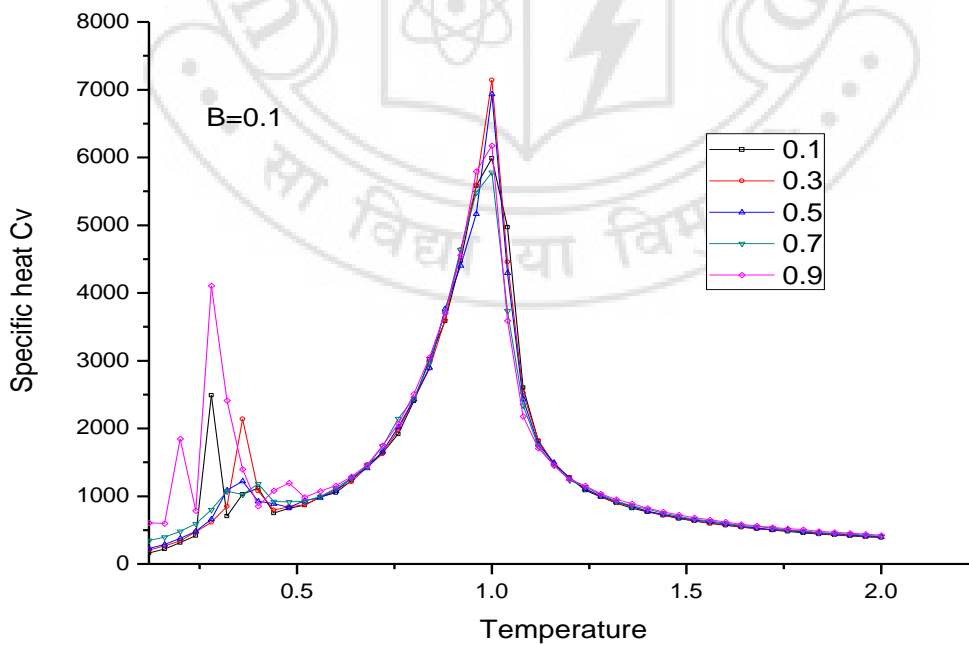


Fig.2.10 Specific heat C_V v/s Temperature for various values of C

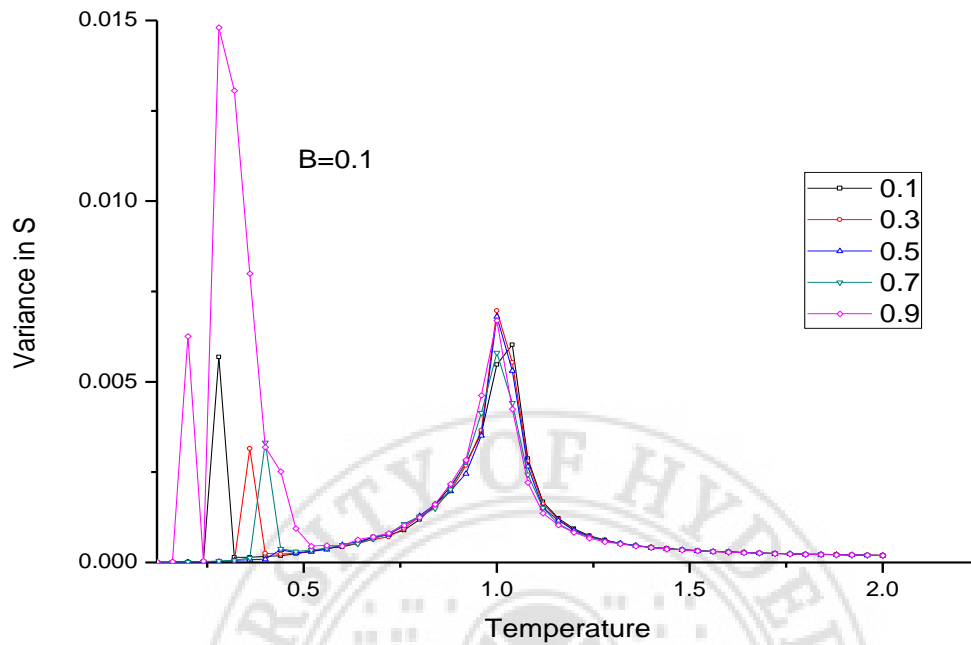


Fig.2.11 Fluctuations in $S (\chi_S)$ v/s Temperature for various values of C

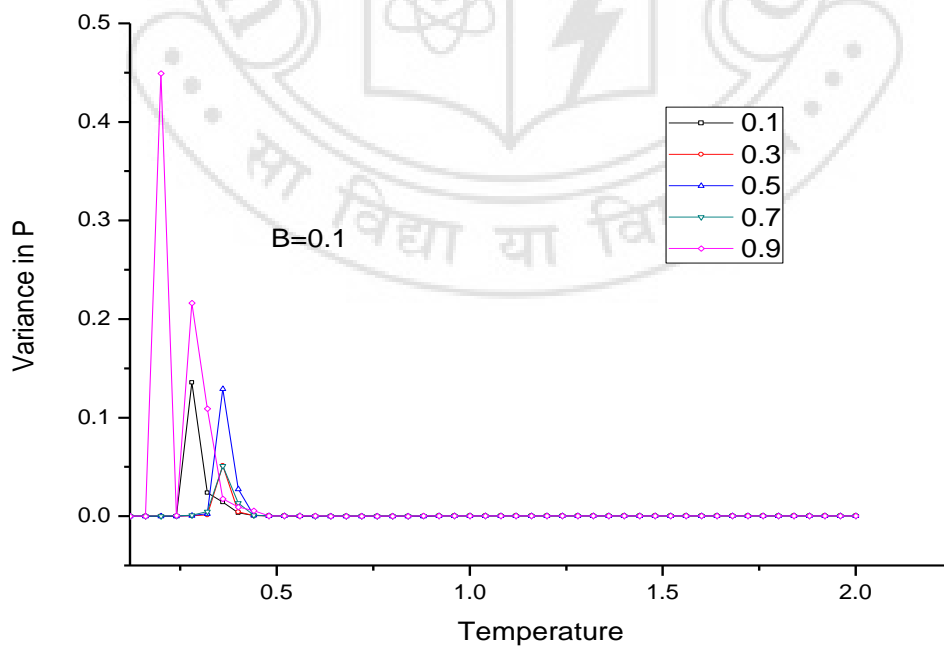


Fig.2.12 Fluctuations in $P (\chi_P)$ v/s Temperature for various values of C

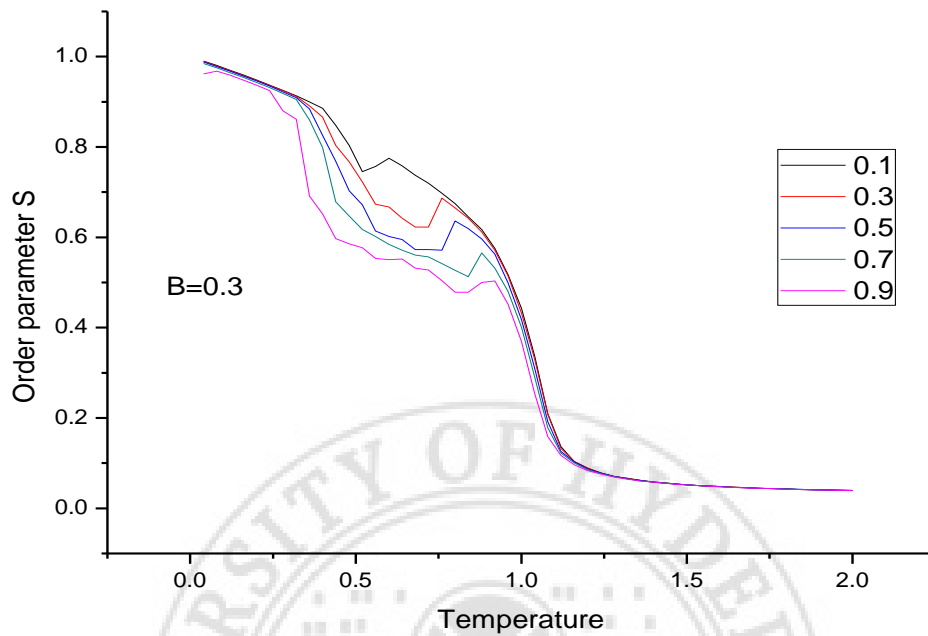


Fig.2.13 Order parameter S v/s Temperature for various values of C

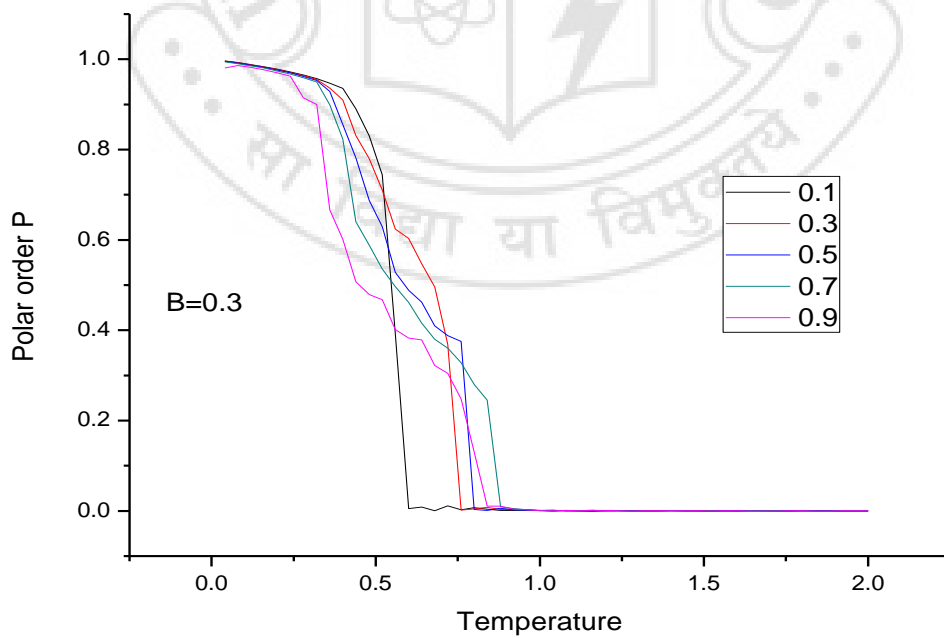


Fig.2.14 Polar order P v/s Temperature for various values of C

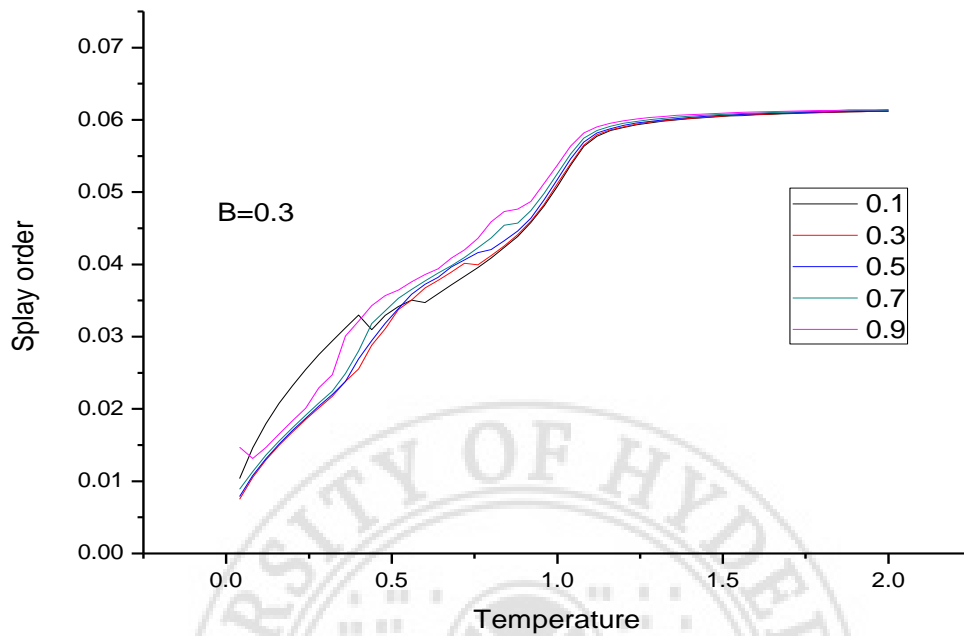


Fig.2.15 Splay order θ v/s Temperature for various values of C

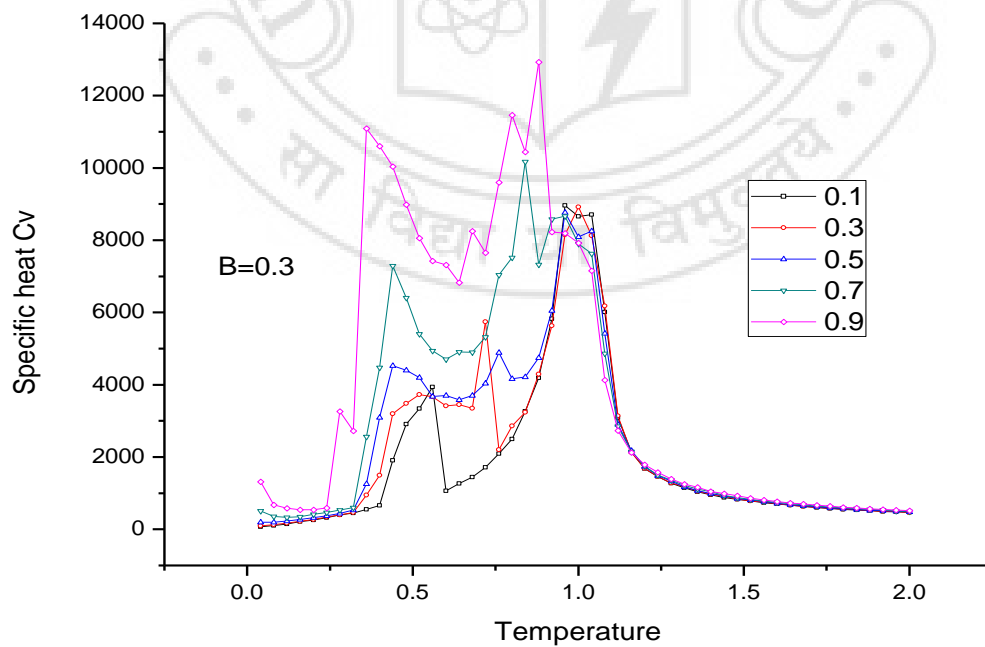


Fig.2.16 Specific heat C_V v/s Temperature for various values of C

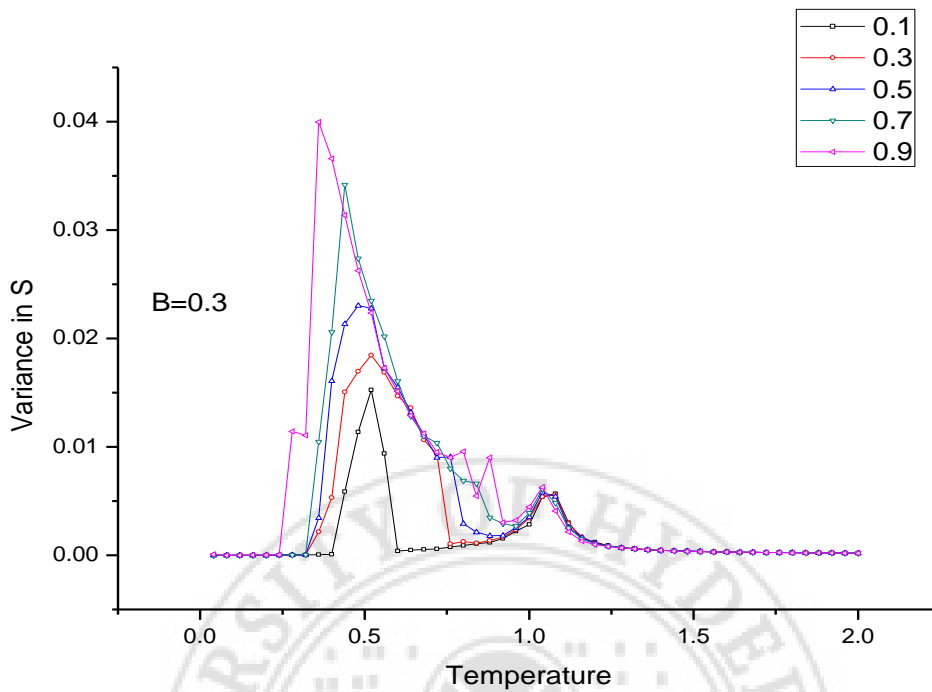


Fig.2.17 Fluctuations in S (χ_S) v/s Temperature for various values of C

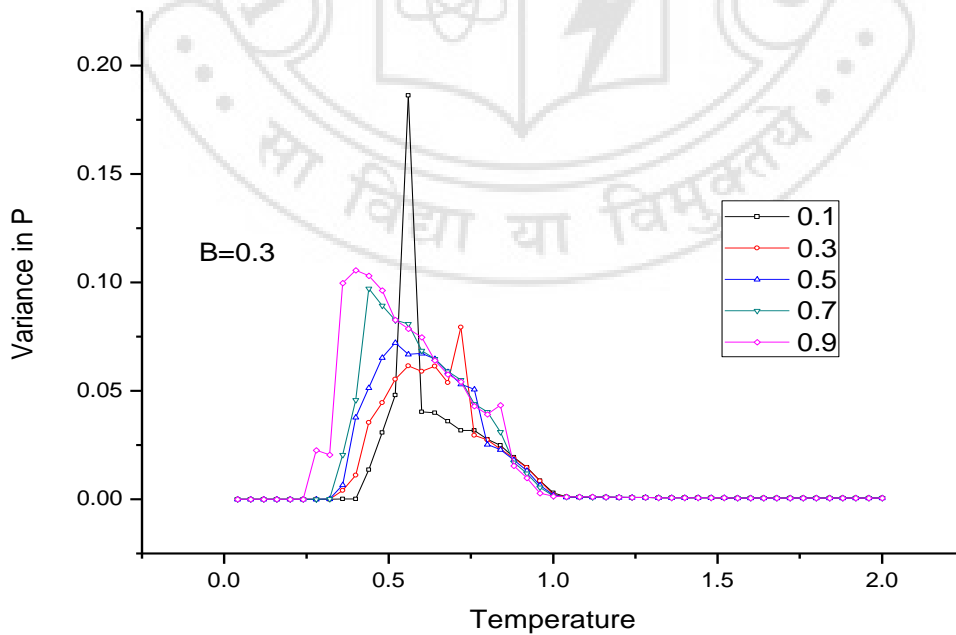


Fig.2.18 Fluctuations in P (χ_P) v/s Temperature for various values of C

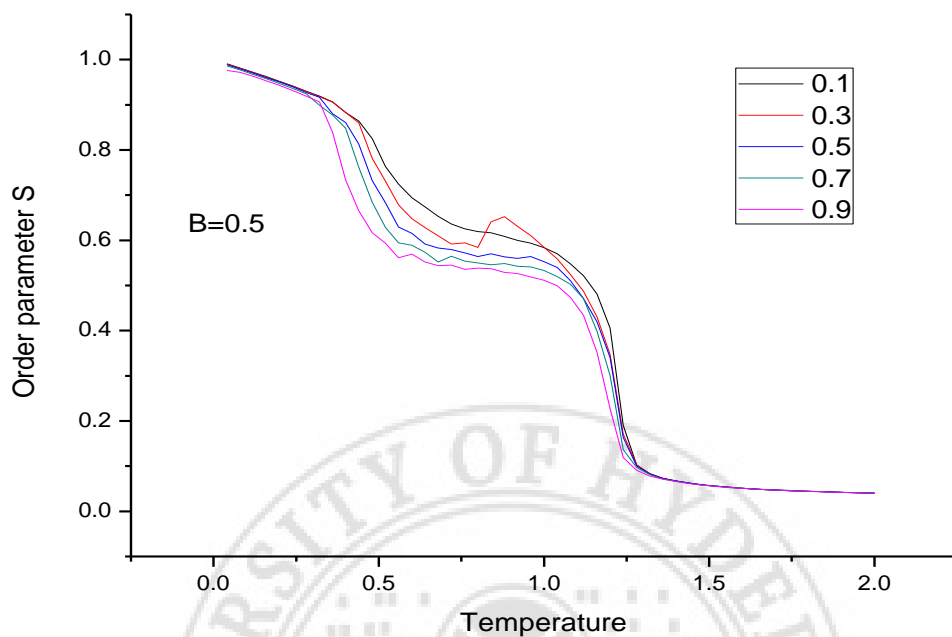


Fig.2.19 Order parameter S v/s Temperature for various values of C

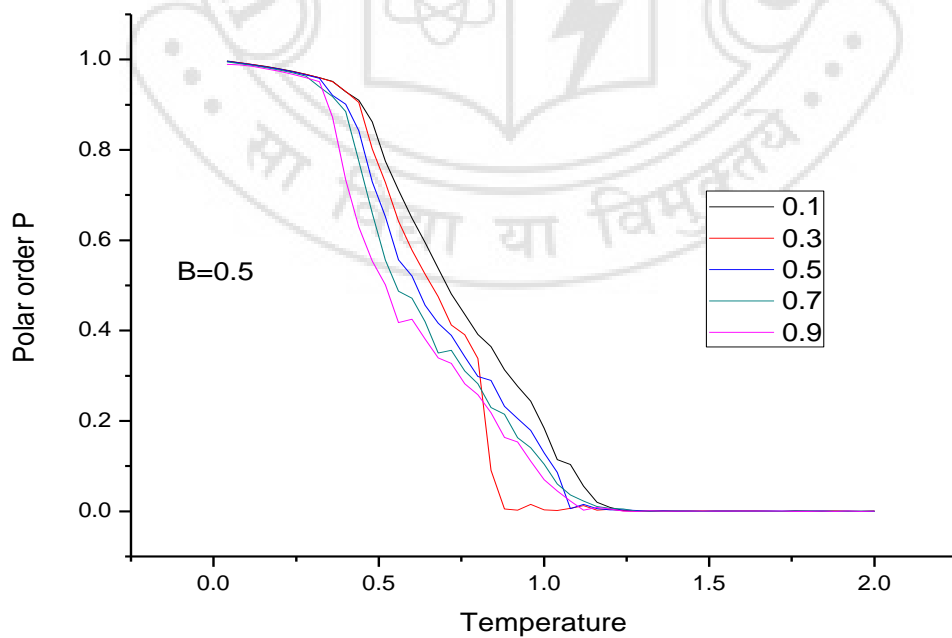


Fig.2.20 Polar order P v/s Temperature for various values of C

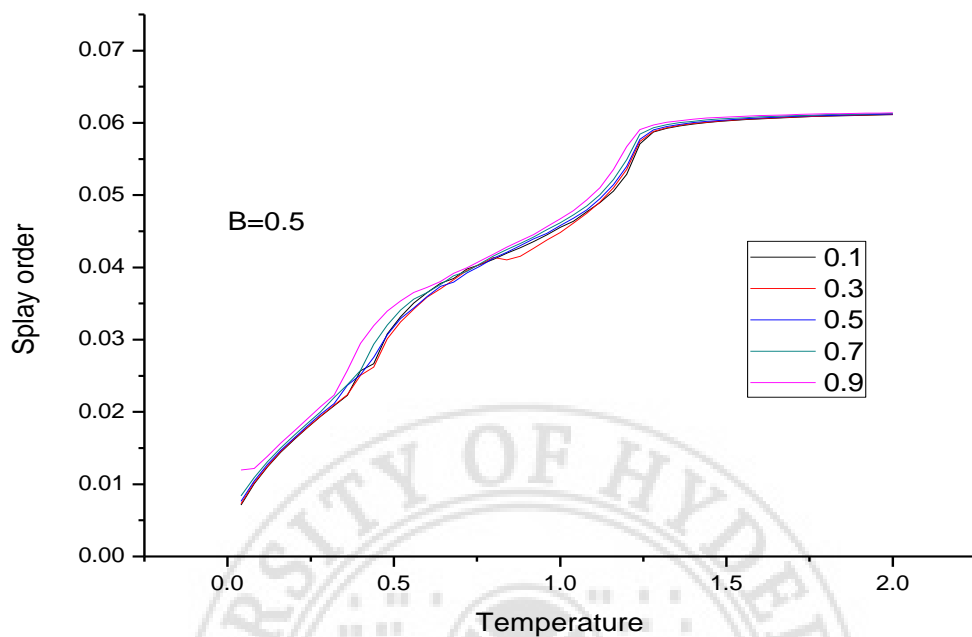


Fig.2.21 Splay order θ v/s Temperature for various values of C

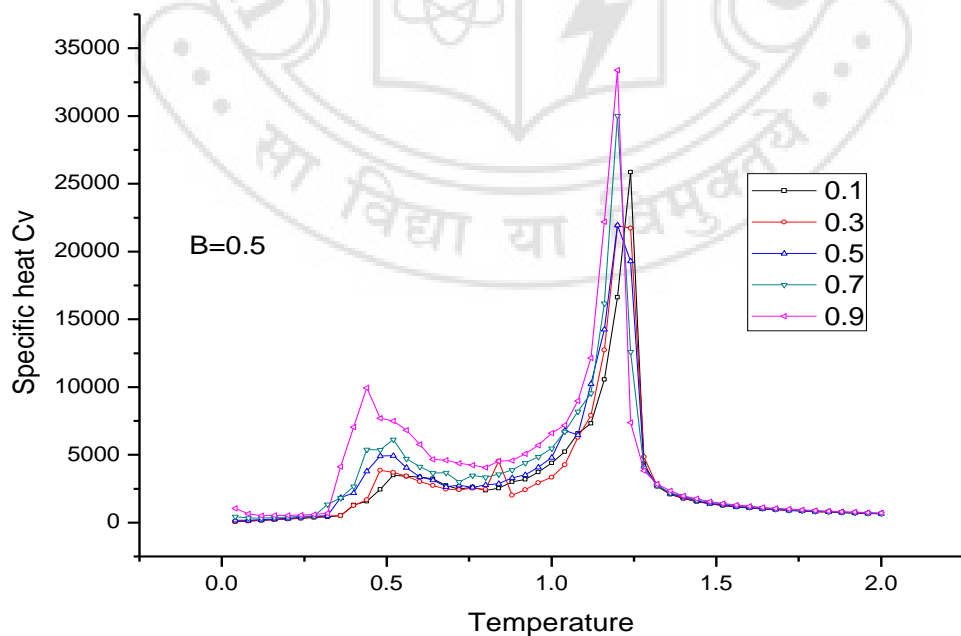


Fig.2.22 Specific heat C_v v/s Temperature for various values of C

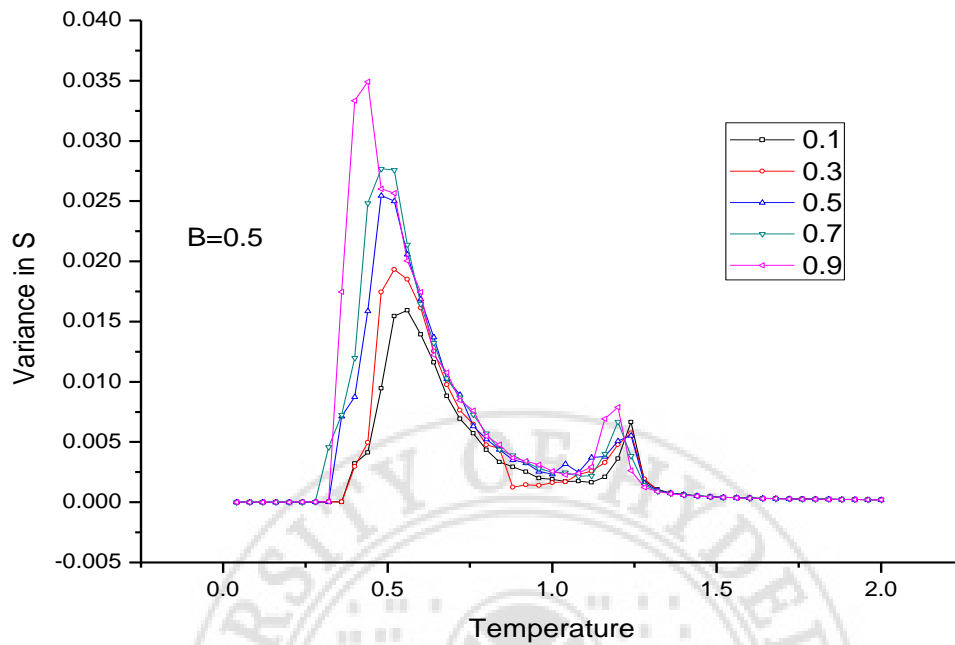


Fig.2.23 Fluctuations in $S (\chi_S)$ v/s Temperature for various values of C

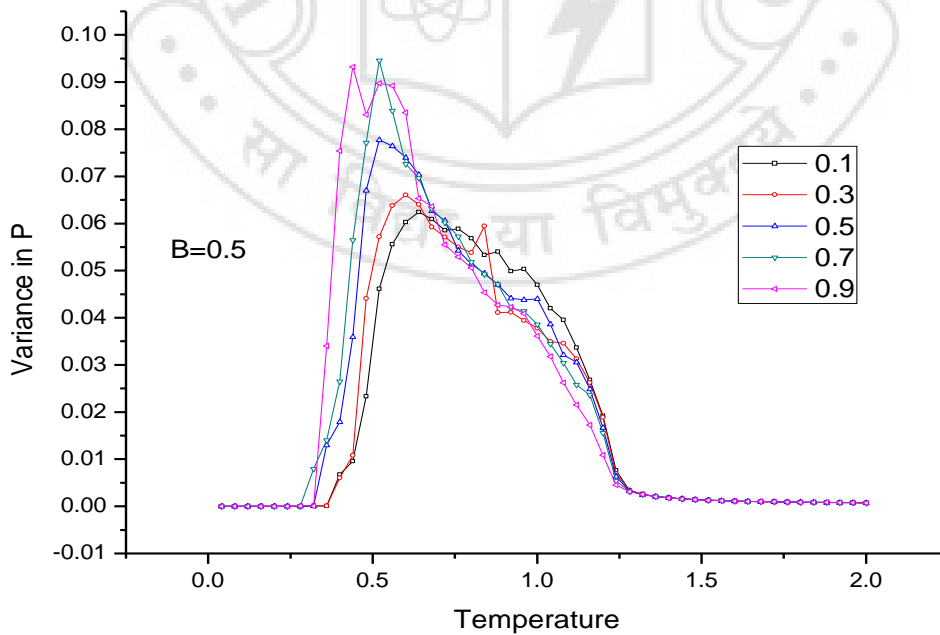


Fig.2.24 Fluctuations in $P (\chi_P)$ v/s Temperature for various values of C

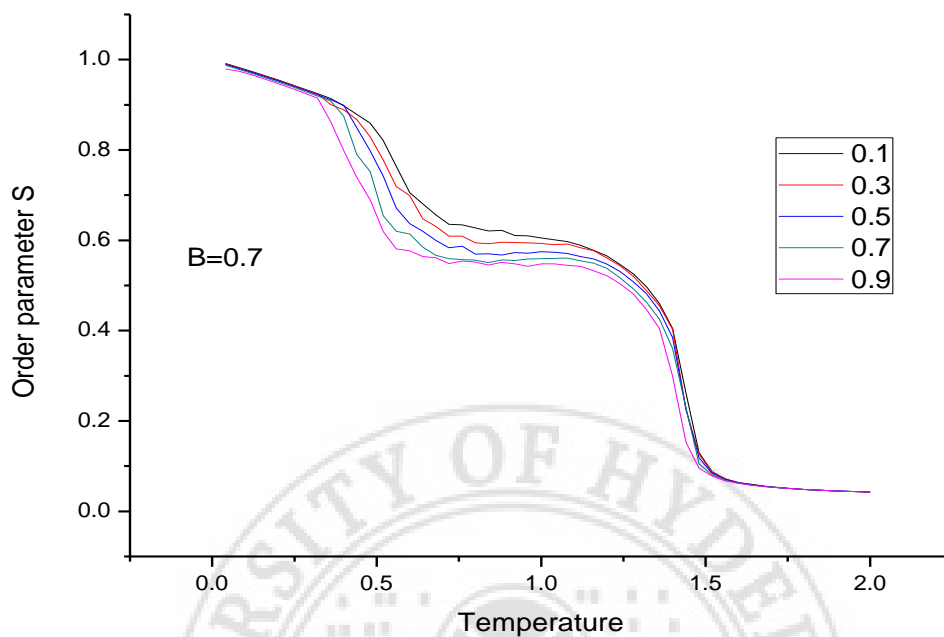


Fig.2.25 Order parameter S v/s Temperature for various values of C

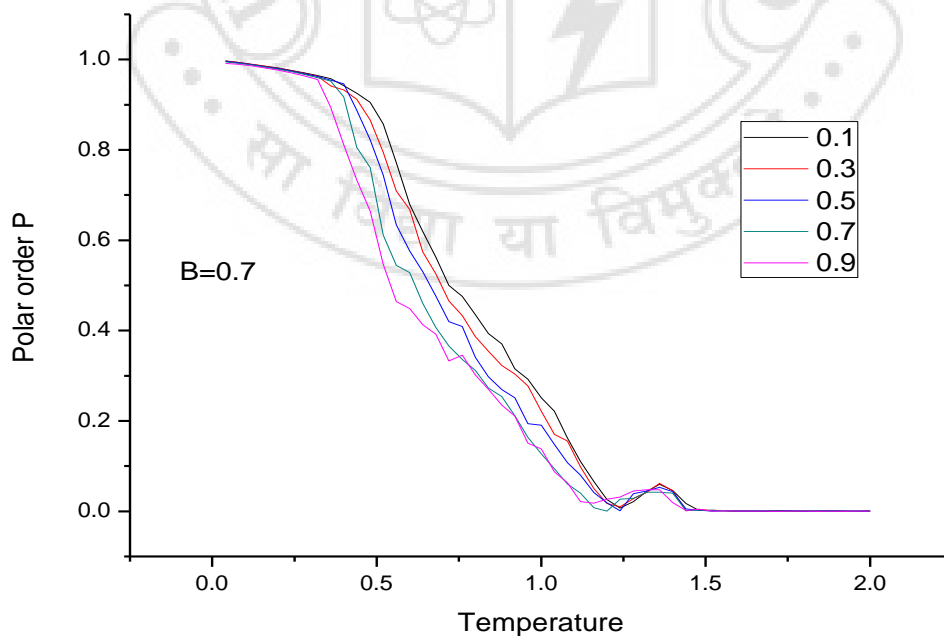


Fig.2.26 Polar order P v/s Temperature for various values of C

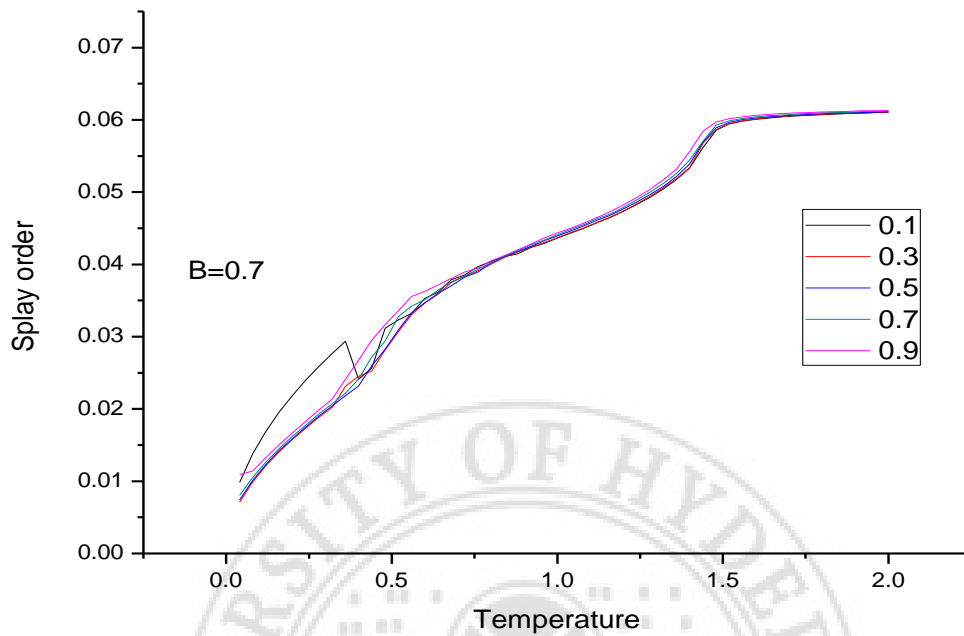


Fig.2.27 Splay order θ v/s Temperature for various values of C

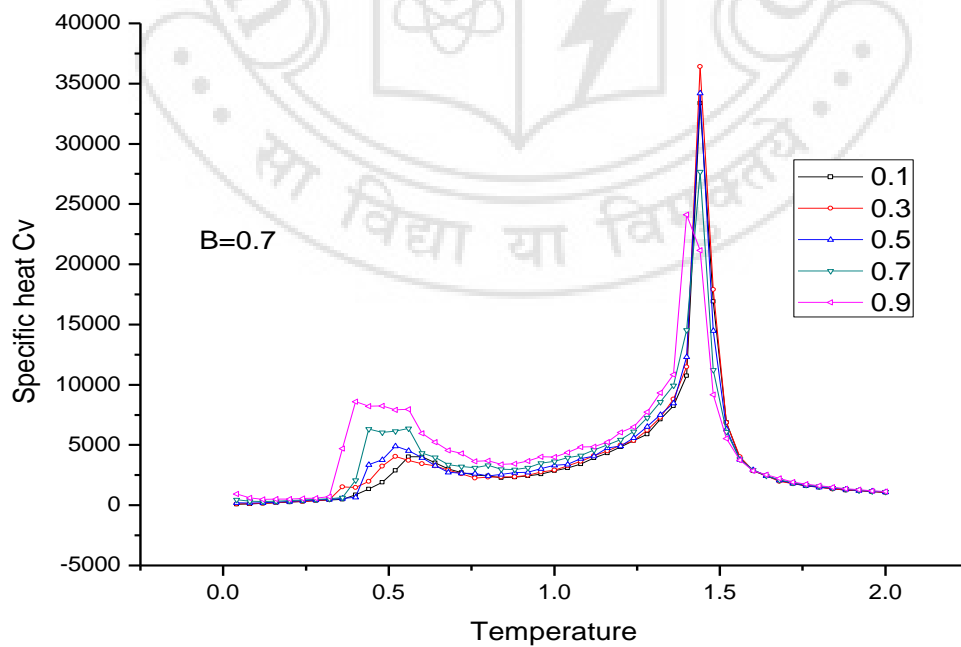


Fig.2.28 Specific heat C_V v/s Temperature for various values of C

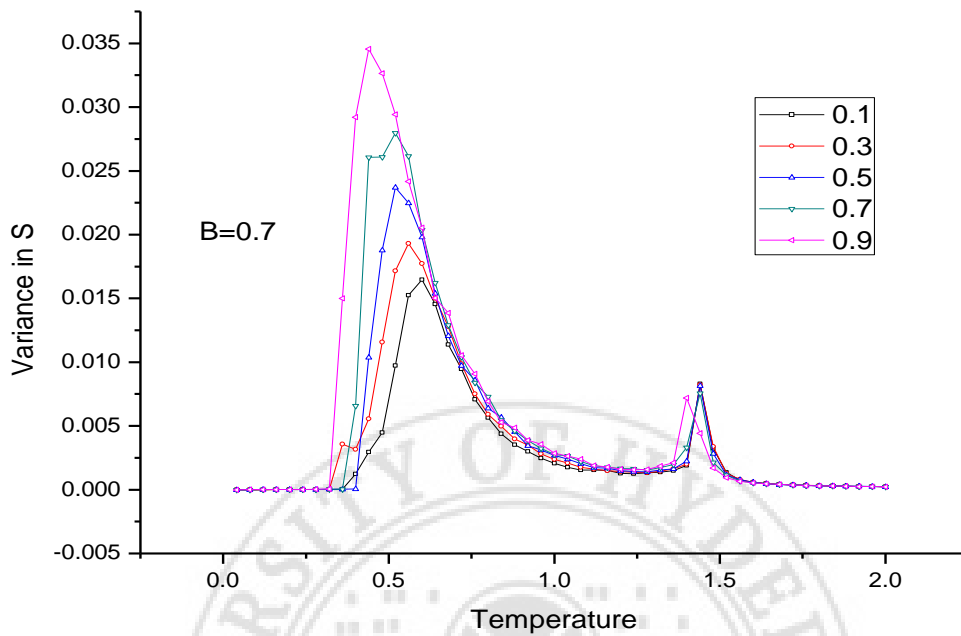


Fig.2.29 Fluctuations in $S (\chi_S)$ v/s Temperature for various values of C

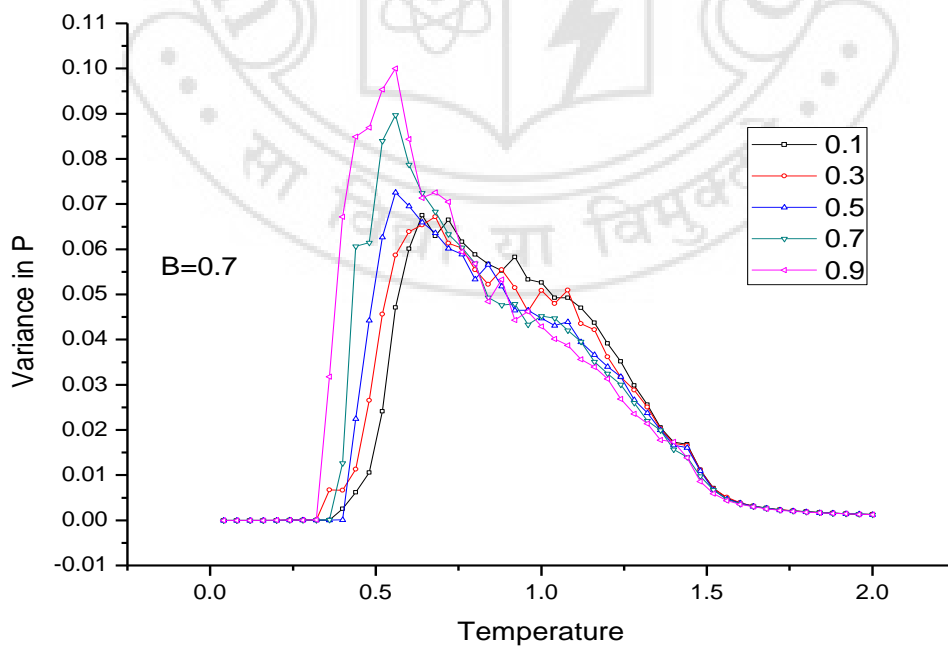


Fig.2.30 Fluctuations in $P (\chi_P)$ v/s Temperature for various values of C

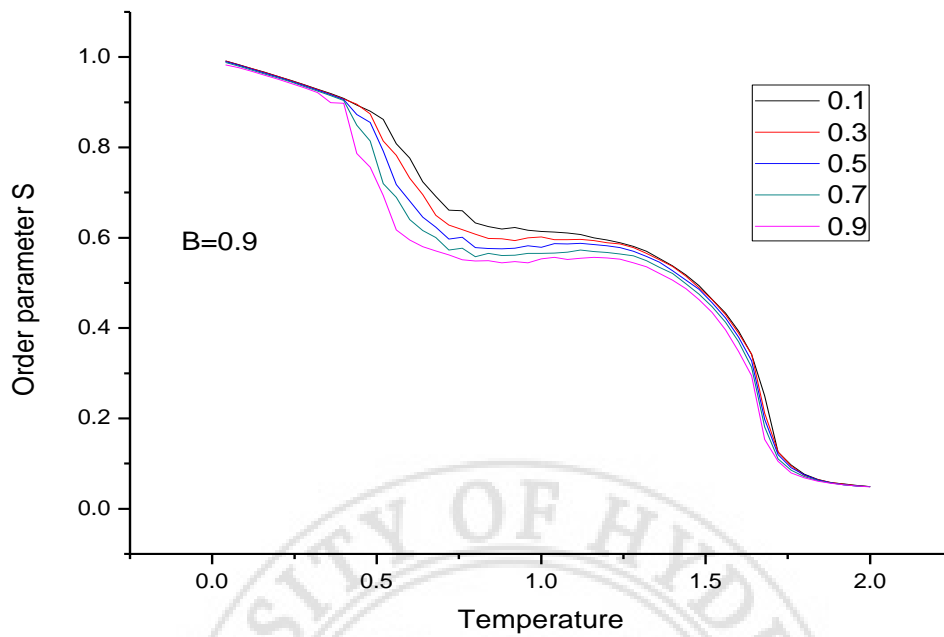


Fig.2.31 Order parameter S v/s Temperature for various values of C

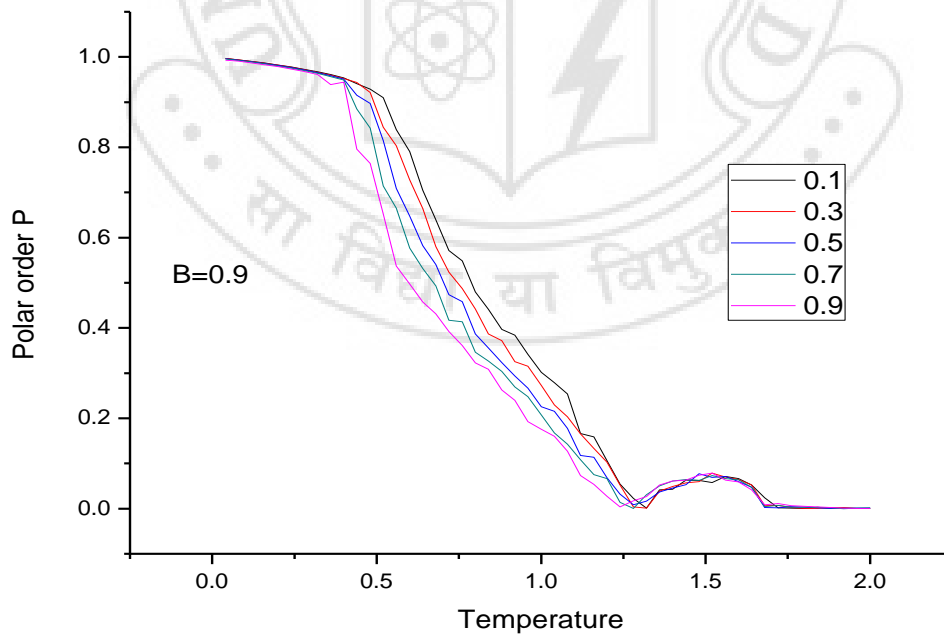


Fig.2.32 Polar order P v/s Temperature for various values of C

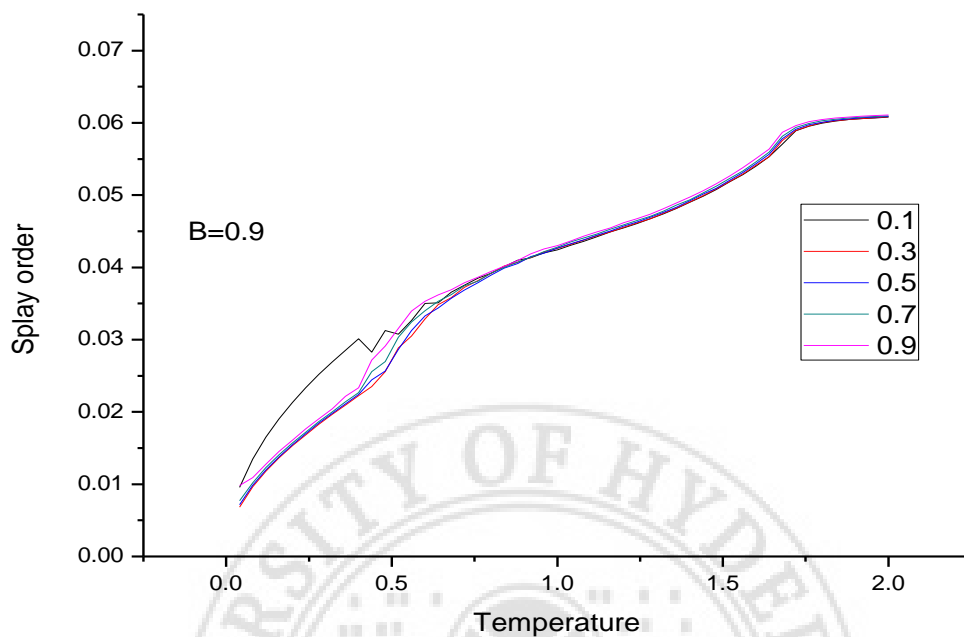


Fig.2.33 Splay order θ v/s Temperature for various values of C

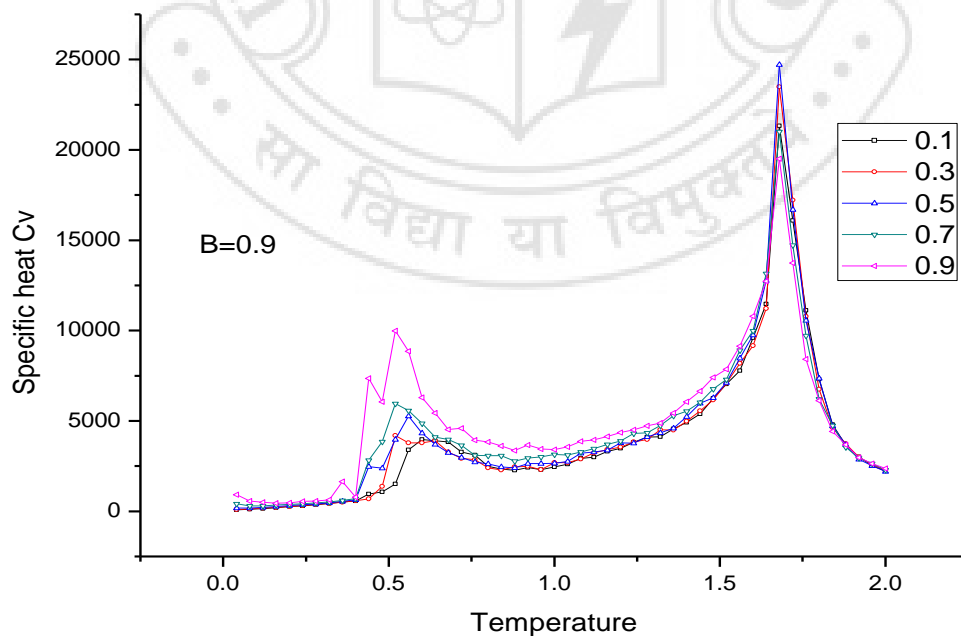


Fig.2.34 Specific heat C_v v/s Temperature for various values of C

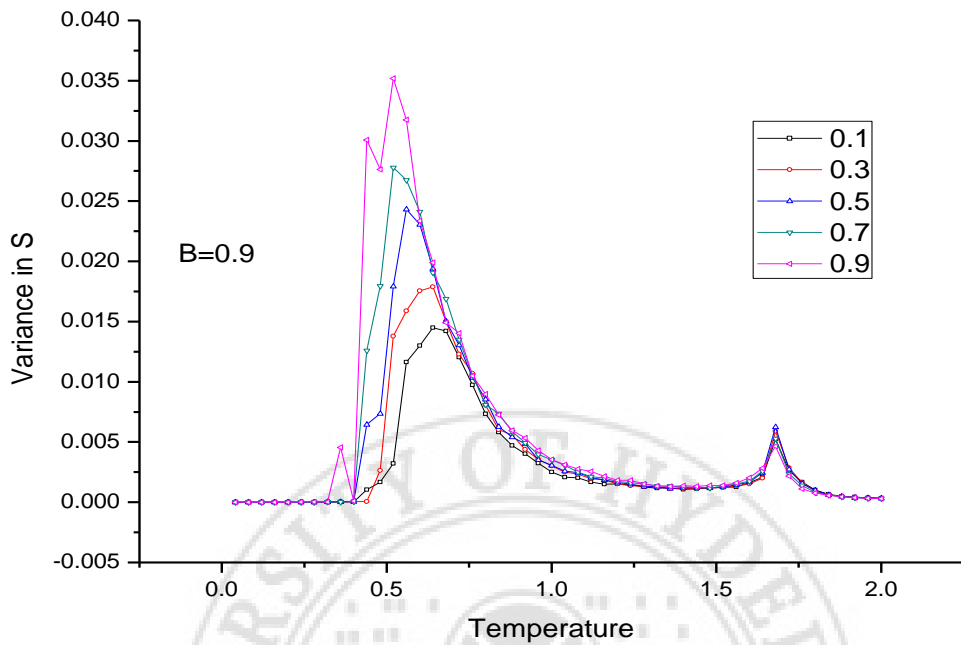


Fig.2.35 Fluctuations in $S (\chi_S)$ v/s Temperature for various values of C

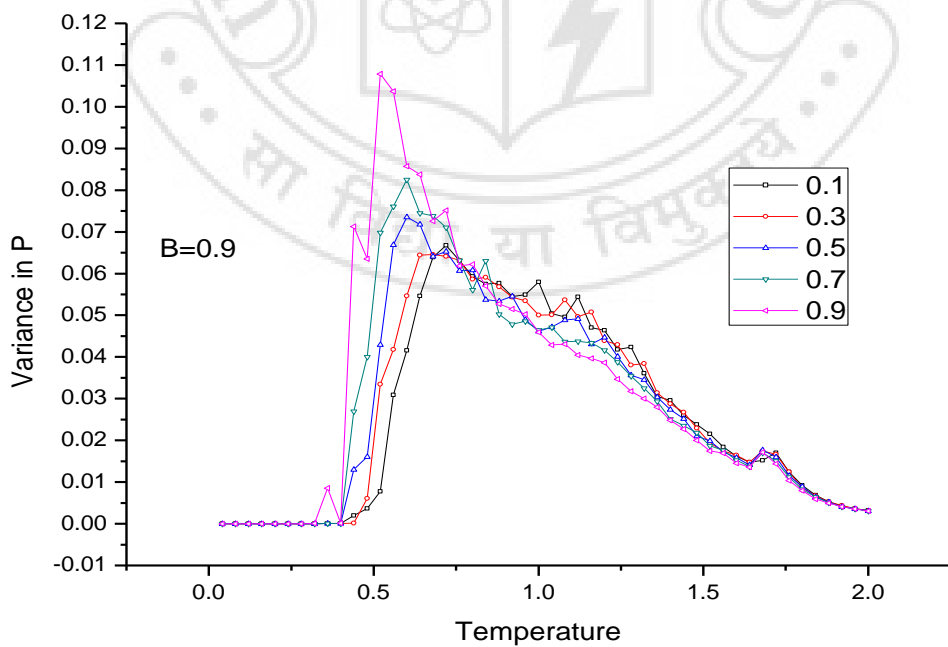


Fig.2.36 Fluctuations in $P (\chi_P)$ v/s Temperature for various values of C

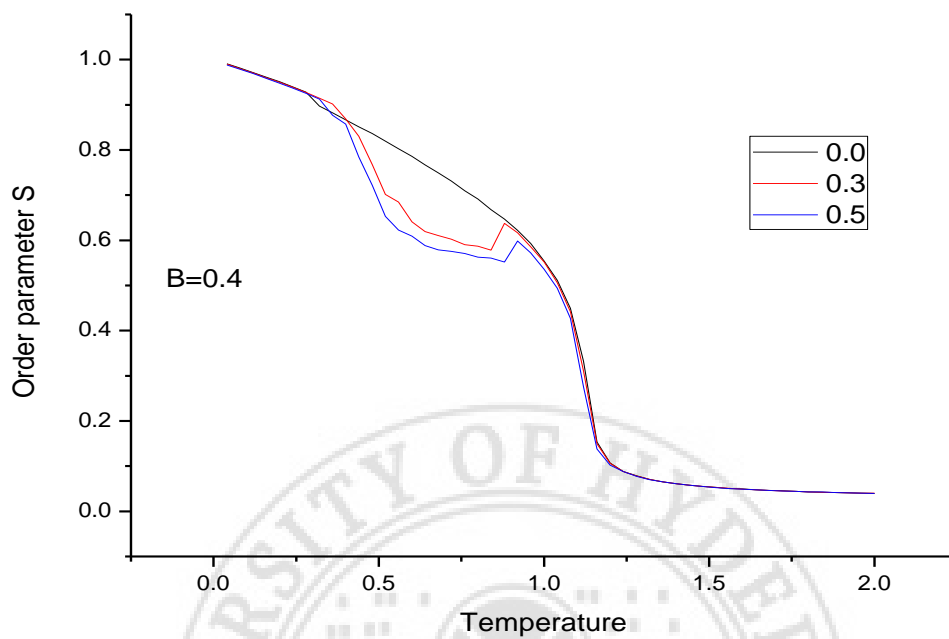


Fig.2.37 Order parameter S v/s Temperature for various values of C

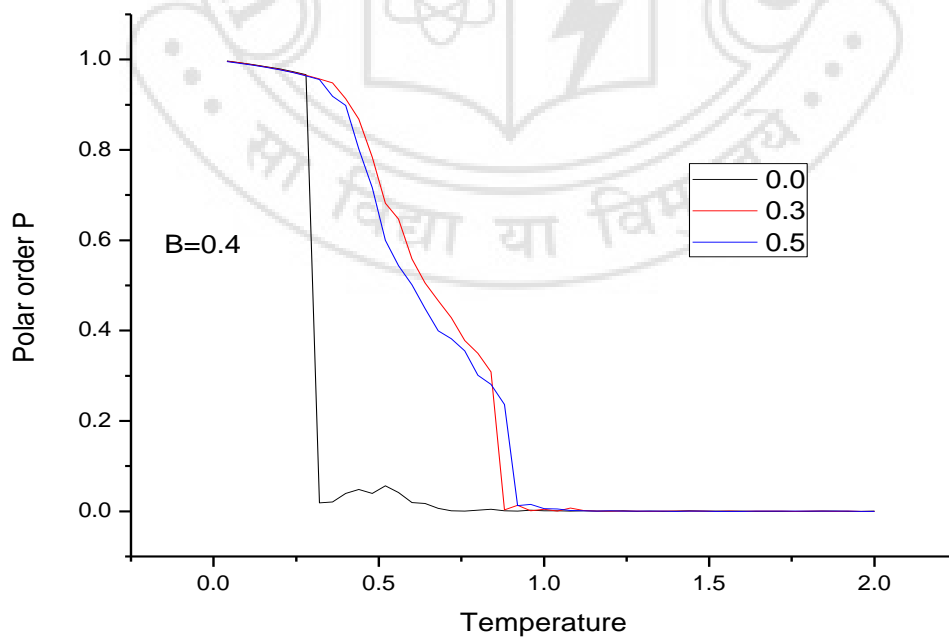


Fig.2.38 Polar order P v/s Temperature for various values of C

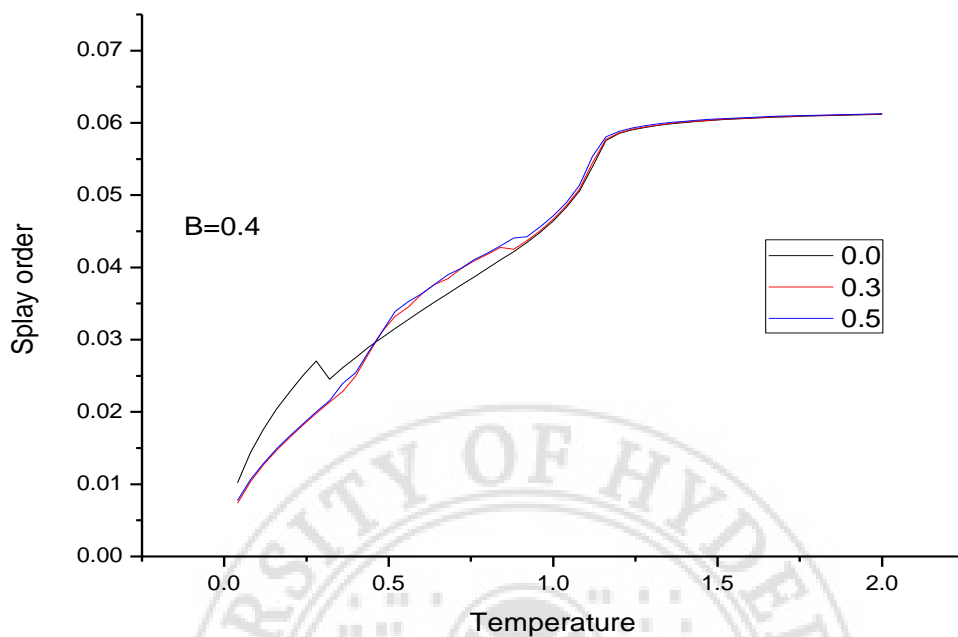


Fig.2.39 Splay order θ v/s Temperature for various values of C

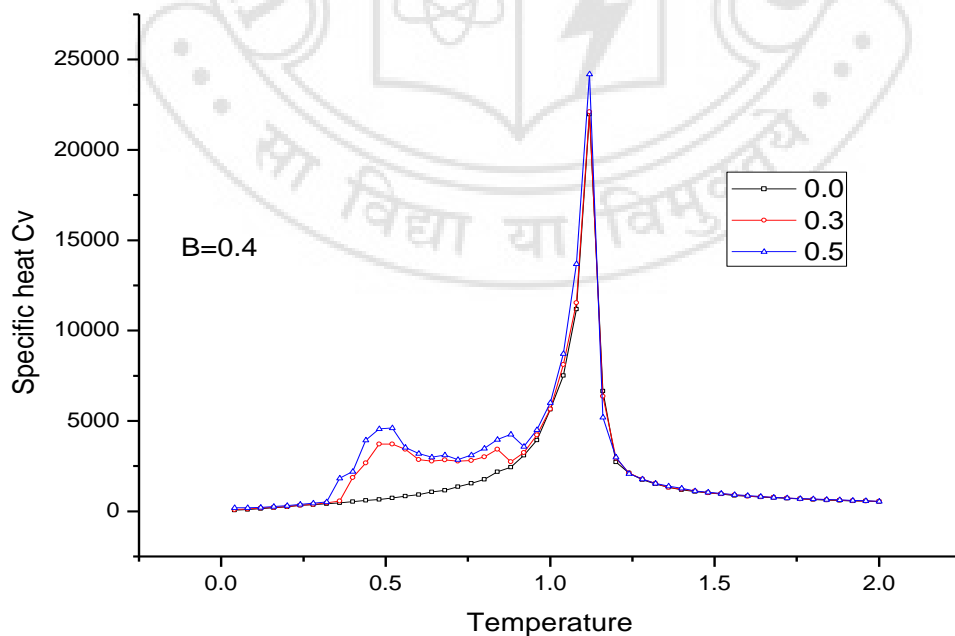


Fig.2.40 Specific heat C_V v/s Temperature for various values of C

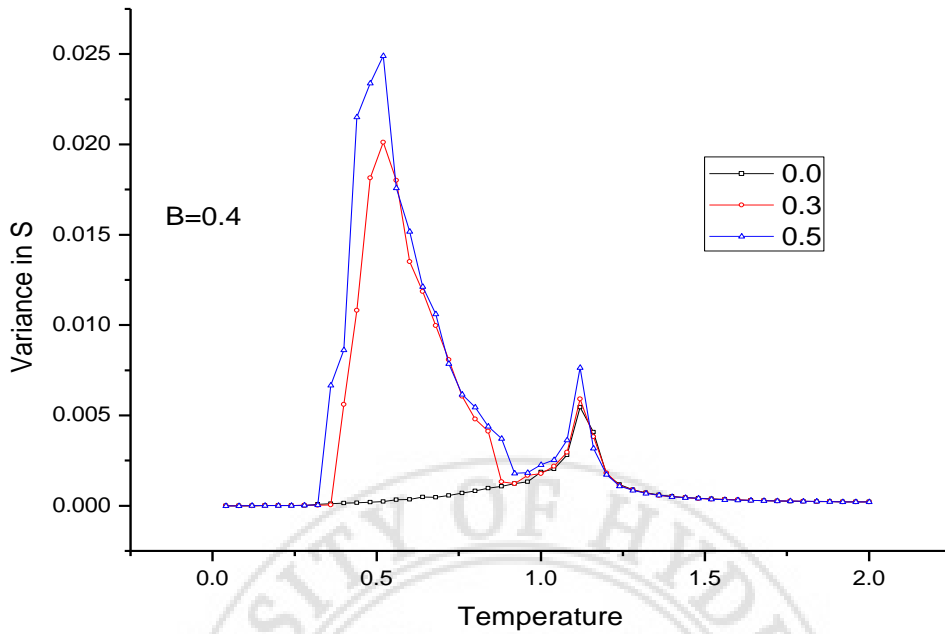


Fig.2.41 Fluctuations in S (χ_S) v/s Temperature for various values of C

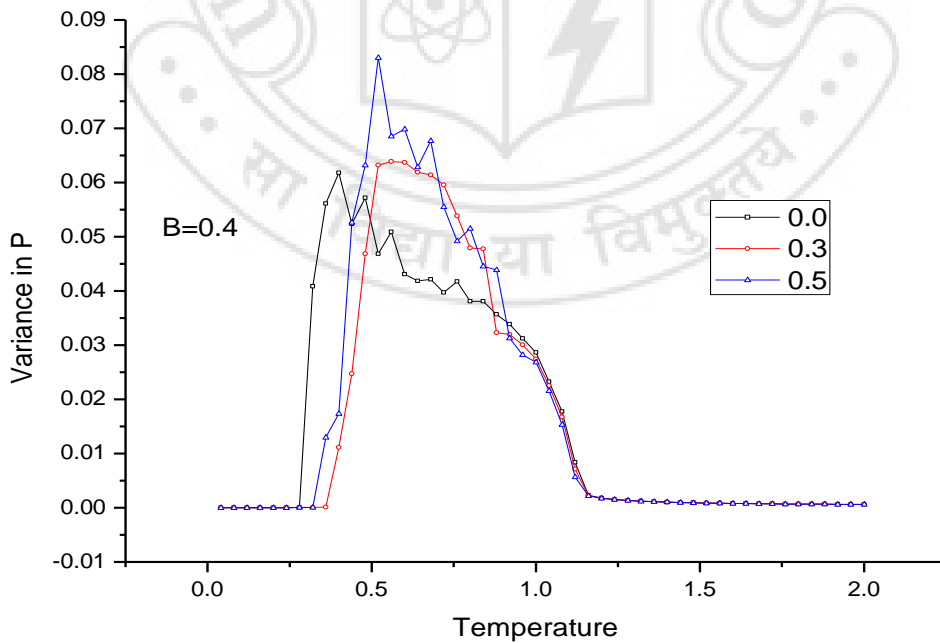


Fig.2.42 Fluctuations in P (χ_P) v/s Temperature for various values of C

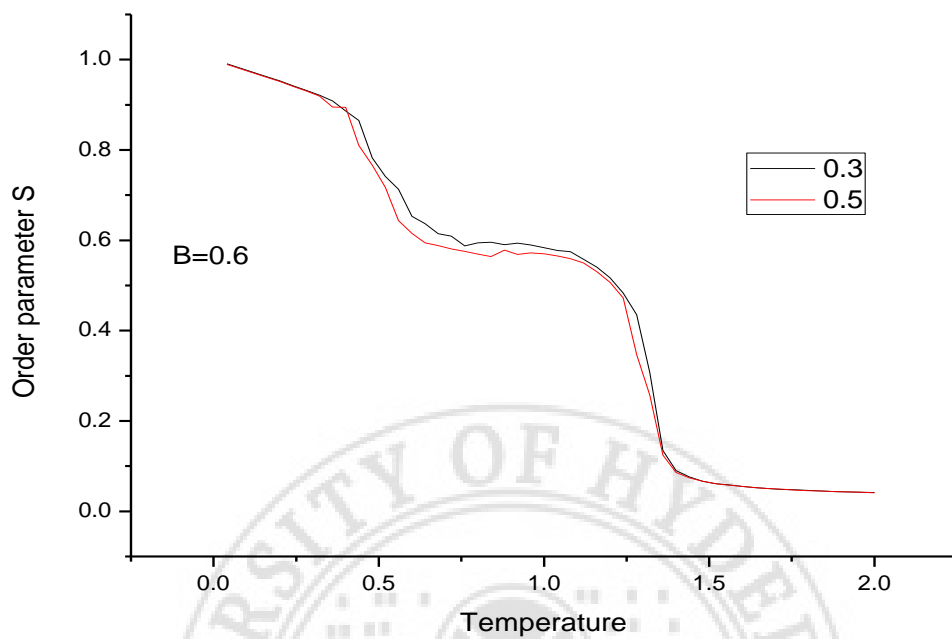


Fig.2.43 Order parameter S v/s Temperature for various values of C

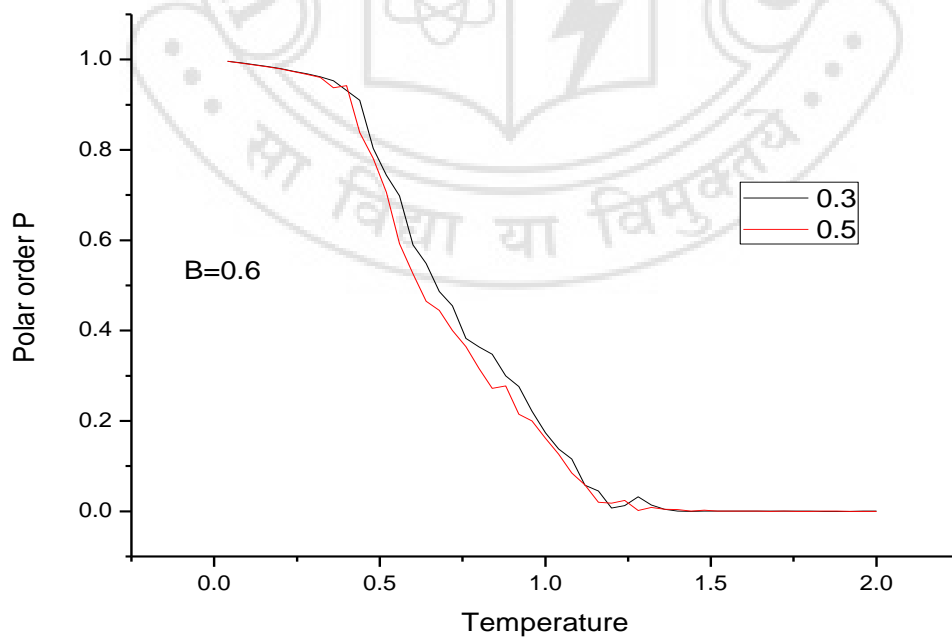


Fig.2.44 Polar order P v/s Temperature for various values of C

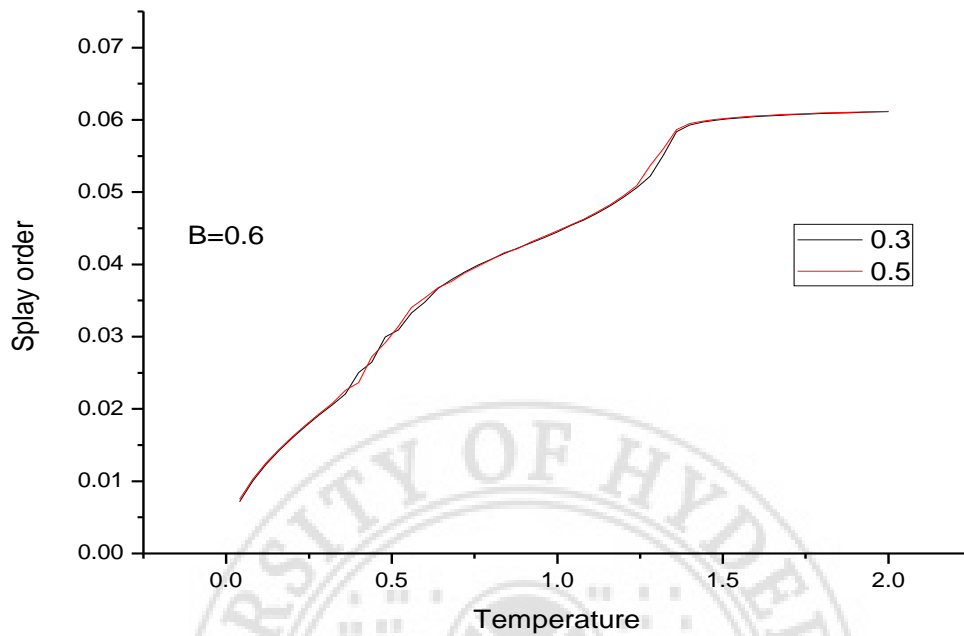


Fig.2.45 Splay order θ v/s Temperature for various values of C

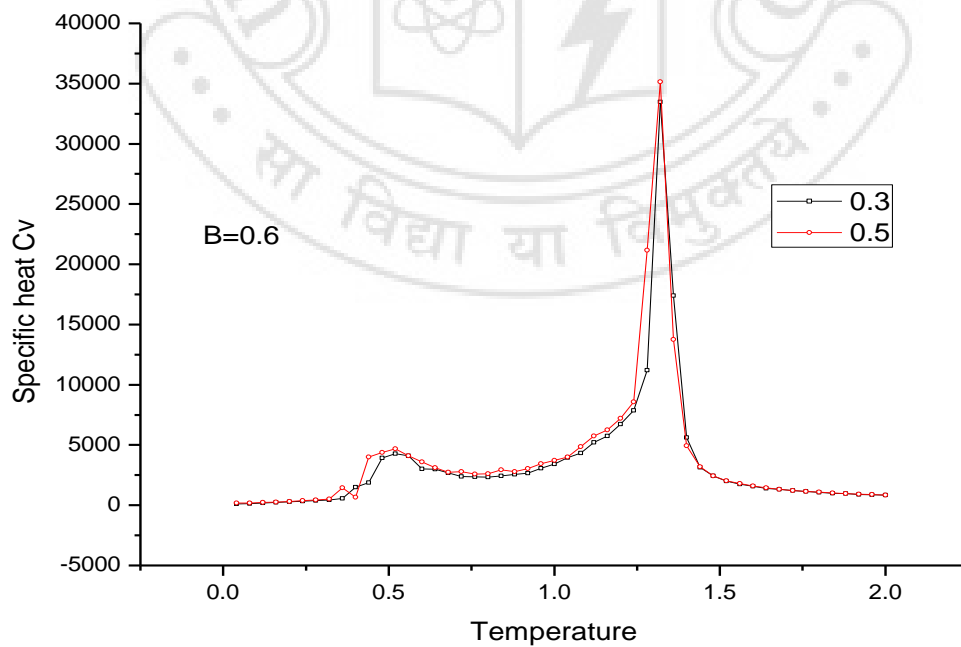


Fig.2.46 Specific heat C_v v/s Temperature for various values of C

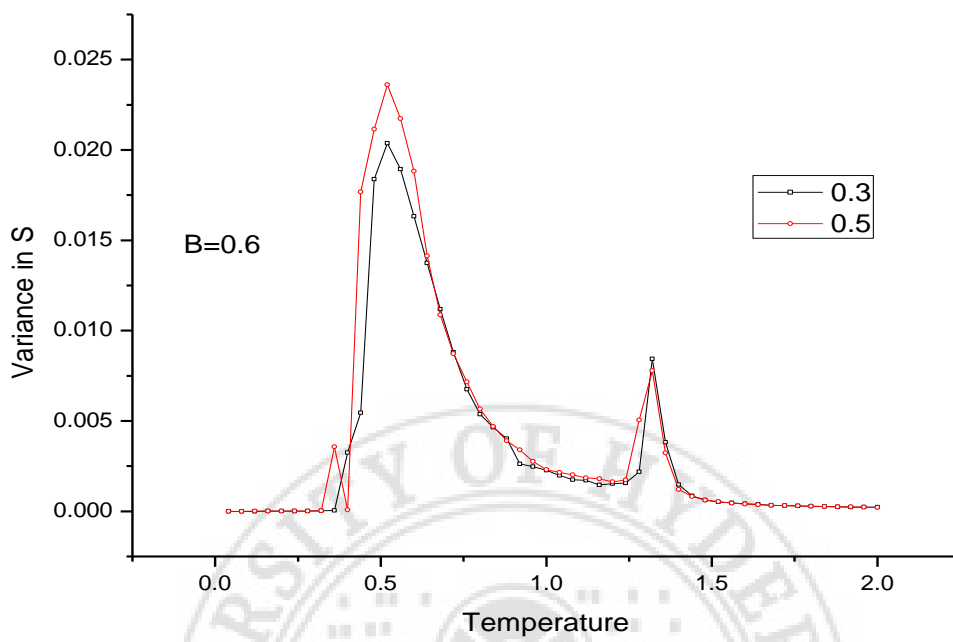


Fig.2.47 Fluctuations in $S (\chi_S)$ v/s Temperature for various values of C

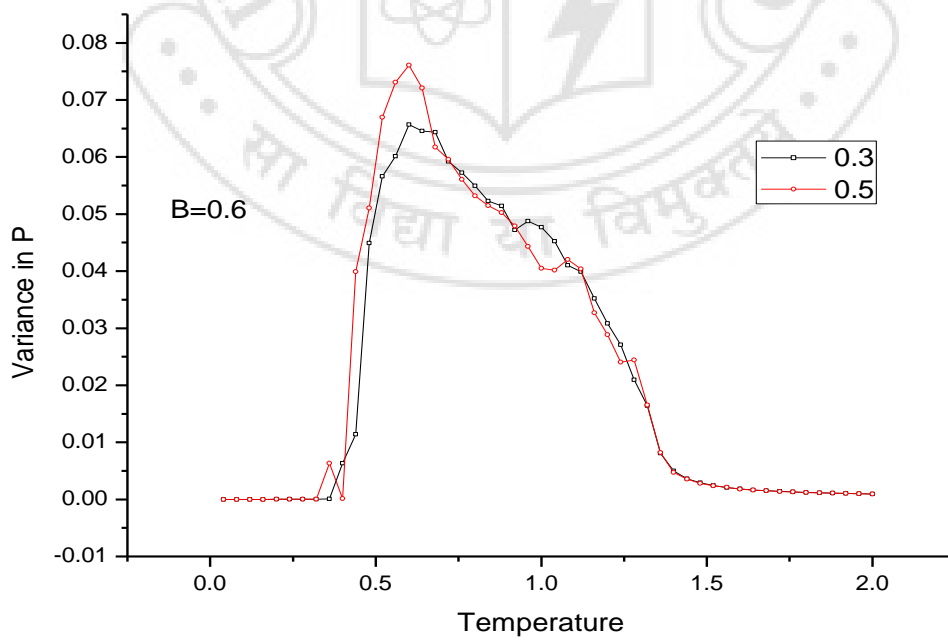


Fig.2.48 Fluctuations in $P (\chi_P)$ v/s Temperature for various values of C

2.5 Discussion

The data in the previous section indicate the nature of thermally induced transition expected of the model Hamiltonian. At the very outset, it may be noted that the results of the earlier simulations [24] differ qualitatively from the present outcome. This point is clarified first before proceeding with further discussion on the consequences of choices of different regions of the parameter subspace [B, C].

It is recalled that the earlier work, in the absence of an external field, predicts [fig.2.6] that at $B=0.09$ and $C=0.03$ [at $A=1.5$, fixed] there interesting transition to occur. At high temperature, approximates corresponding to the LL model (i.e. near $T\sim 1.1$) an isotropic to nematic transition takes place with S building up gradually. The polar order P and splay order θ are zero. This is followed up subsequently on cooling by the onset of polar order (P abrupt jumps to a non-zero value), and also a splay order (θ abruptly changes from zero to small value ~ 0.05). This polar transition has leads to an abrupt dip in the value of S . On further cooling, the scenario is that the polar order is quite high, the orientational order recovers to about 0.7, the splay order remains saturated. Our results do not tally with this outcome. We find out that S does not dip [fig 2.7, plot corresponds to $C=0.3$], P shows a sharp increase [fig 2.8, $C=0.3$], and the splay order actually starts dipping from about $T \sim 1.1$ [fig 2.9, $C=0.3$]. An important qualitative difference is that S never below P , and there is no onset of a splay transition.

Next we compare the earlier results (field zero) at $B=0.4$ and $C=0.3$ with our data (fig 2.37, $C=0.3$; fig 2.38, $C=0.3$; and fig 2.39, $C=0.3$). The earlier simulations predict simultaneous on set of orientational order S , polar order P , and splay order θ at same (high) temperature ($T\sim 1.12$). We report differently: orientational order S sets in at $T \sim 1.1$, polar order sets in at $T \sim 0.84$ (and there is a small dip in S in the initial stages of the onset of P), and of course the presence of splay order is not observed. Repeated verification of our results constrains us to suggest that our prediction differ from earlier work even qualitatively.

Next we compare our own data for different sets of [B, C] values with the help of both phase diagrams of S and P , as well also by examining the fluctuation behaviour in the system (C_V , χ_S and χ_P). It may be noted that for the fixed value of A in the Hamiltonian

(constant background of interactions promoting uniaxial nematic order through apolar interactions), the role of B and C in a way competing. While B term quantitative the energy gain by making the (pear shaped) molecules develop a cooperative vector order parameter, the C term indicates the energy expenditure by such a symmetry-breaking cooperatively due to consequent spontaneous splay distortion. Thus comparisons of the effects of B and C terms in the following discussion have this underlying physical consequence.

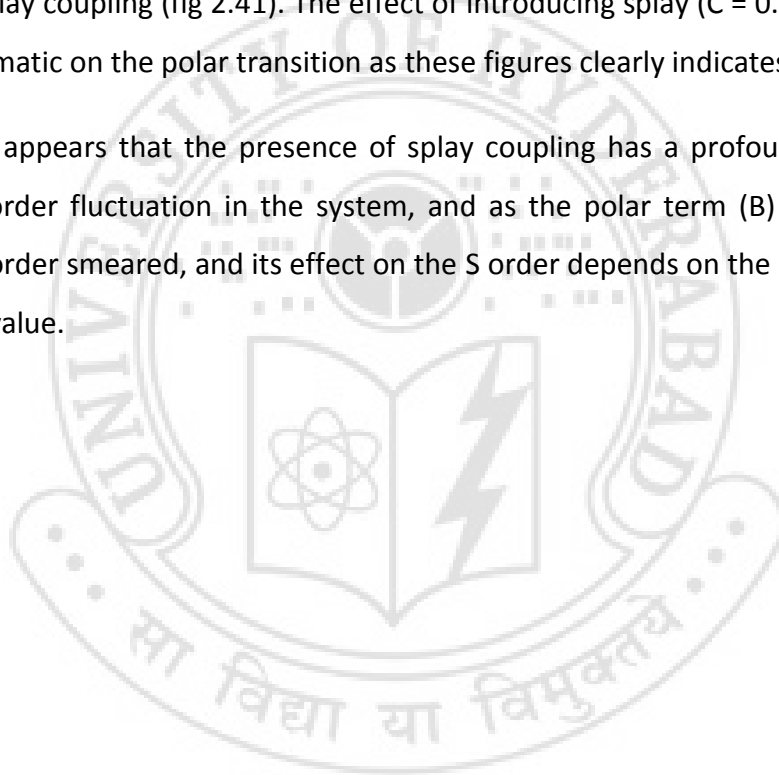
In this sense, the variation of splay term (from $C=0.1$ to 0.9) at $B=0.1$ (small polar perturbation) does not lead to any curious results, but for nematic ordering transition at about $T \sim 1.0$ (fig 2.7), a polar transition at about $T \sim 0.4$ (fig 2.8) which shifts slightly with changes in the splay contribution. In all the cases we do not find a splay transition, and so will not discuss this variable any further, and for the sake of records its variation presented in all the cases studied in appropriate figures (Table–1 for details). The actual temperature where the transitions are observed, as measured within the temperature resolution of the simulation ($\Delta T \sim 0.04$) from the fluctuation peaks are summarized in Table-2. The C_V peaks are strong at the nematic transition, and weak at the polar transition. χ_S shows two peaks at the two transitions, while χ_P exhibits divergence only at the low temperature transition. The case of $C = 0.9$ (with $B = 0.1$) is unusual wherein the splay contribution does not permit a systematic variation and onset of polar order.

The case of $B = 0.3$ is qualitatively different (Figs 2.13 – 2.19). S shows a dip coincident with polar transition, and this transition temperature depends on the value of C . The C_V profile that the process of formation of a polar nematic might even involve curiously these stages (fig 2.16). Interestingly the χ_S has the larger fluctuation near the low temperature transition, rather than IN transition at higher temperature. The sharp transition features of the polar order yield to a study increase at $B = 0.5$. At this B value the polar transition seems to the softening (fig 2.20), as is evident from the evolution of S (fig 2.19) with a smooth variation but for at $C = 0.3$. C_V peak is strong at the nematic transition (fig 2.22) , while χ_S and χ_P have stronger signatures at the polar transition (fig 2.23 and fig 2.24).

The case of $B = 0.7$ and 0.9 are characterized by higher temperature for the nematic transition ($T \geq 1.5$), (see figs 2.25 and 2.31), a curious transient build-up of polar order

immediately below the corresponding IN transition (fig 2.26 and 2.32), and a general smearing out of the polar transition. These are supported by the strong C_V peak at IN transition and the small peaks at the polar transition. The corresponding variation of χ_S and χ_P are consistent with this description. Finally, we compare the case of $B = 0.4$ with and without C term; we would like to contrast the transition sequence with appreciable polar coupling, but with and without splay perturbation. Referring to figs. 2.37 – 2.42, one find that $C = 0.0$, S varies quite smoothly with only a small hint of a polar transition at about $T \sim 0.3$. Polar transition is strong (fig 2.38) and C_V does not show the effect of polar transition (fig 2.40). It is equally interesting that χ_S also is insensitive to the polar transition in the absence of a splay coupling (fig 2.41). The effect of introducing splay ($C = 0.3$ and 0.5), at $B = 0.4$ is quite dramatic on the polar transition as these figures clearly indicates.

Thus it appears that the presence of splay coupling has a profound effect on the energy and S order fluctuation in the system, and as the polar term (B) is increased the onset of polar order smeared, and its effect on the S order depends on the relative values of C, at a given B value.



Chapter 3:

Conclusions

We examine the model Hamiltonian proposed recently was investigated with a view to examining its applicability as a function of temperature and we observed that the results were differ qualitatively from our present work. The order parameter S does not dip for the value of $B = 0.1$ and $C = 0.3$, the polar order P shows a sharp increasing and the splay order start dipping from about $T = 1.1$. In this we does not observed the any considerable splay transition thought the temperature range we studied.

In our project we considered the study of the consequences of variation of parameters B and C over a 30 combinations in the above Hamiltonian model, looking for changes in the thermal behaviour of the system, and the resulting phase diagram. We observed that the transition temperature of order parameter S are in good agreement with the all values of C varying from 0.1 to 0.9 for $B = 0.1$. For $B = 0.3$, the IN transition at high temperature is in good agreement with the reported results, but at low temperature it shows a dip at polar transition. For further values of $B = 0.5, 0.7, 0.9$ there is a smooth variation in S (except for $B = 0.5, C = 0.3$), and we find two transitions one at lower temperature near polar transition and one at IN transition. The polar order P , transition is very sharp at lower value of B i.e. 0.1 and this sharpness smeared out as we increase the B from 0.3 to 0.9, and also we observed there is a transition at higher value of $B = 0.7$ and 0.9. Except at $B = 0.3$, we observed the C_V peaks at two different places at the transition temperatures of the polar (smaller fluctuations) and nematic (larger fluctuations) phases, but at $B = 0.3$ we observed large fluctuations in between the transition temperature of polar and nematic. As we increase the value of B the fluctuations in S (χ_S), have large fluctuations at transition temperature of P compare to fluctuations near transition temperature of S . The fluctuations in P (χ_P), for lower value of $B = 0.1$ is sharp for all the values of C , and also sharp for $B = 0.3$ and $C = 0.1$, but further increasing the value of B this sharpness become broad, and this broadness is increase with increasing the value of C . In all the values of subspace $[B, C]$, we do not observed any splay transition. We also observed the variation of $B = 0.4$ for no

splay contribution i.e. $C = 0.0$, the S varies smoothly and shows a small bent at $T = 0.3$, and remaining values of B and C shows the same nature as we observed above.

We conclude that that the presence of splay coupling has a profound effect on the energy and S order fluctuation in the system, and as the polar term (B) is increased the onset of polar order smeared, and its effect on the S order depends on the relative values of C , at a given B value.



References:

1. F. Reinitzer Montash, Chem. 9, 421 (1888).
2. G. Friedel, Ann. Physique. 18, 273 (1922).
3. P. G. de Gennes, *Physics of Liquid Crystals Oxford* (1976).
4. Meyer, R. B., 1969, Phys. Rev. Lett., 22, 918.
5. J. Prost and J. P. Marcerou, *J. Phys (Paris)* 38, 315 (1977).
6. L. M. Blinov and V. G. Chigrinov, *Electrooptic Effects in Liquid Crystals* Springer, New York (1993).
7. C. Denniston and J. Yeomans, Phys. Rev. Lett. 87, 275505 (2001).
8. A. J. Davidson and N. J. Mottram, Phys. Rev. E 65, 051710 (2002).
9. J. S. Patel and R. B. Meyer, Phys. Rev. Lett. 58, 1538 (1987).
10. M. Cepic and B. Zeks, Phys. Rev. Lett. 87, 085501 (2001).
11. A. G. Petrov, Biochim. Biophys. Acta 85535, 1 (2001).
12. S.T.Lagerwall, *Ferroelectric and Antiferroelectric Liquid Crystals* (1999).
13. P. R. M. Murthy, V. A. Raghunathan, and N. V. Madhusudana, *Liq. Cryst.* 14, 483 (1993).
14. A. G. Petrov, D. A. Dunmar, A. Fukuda, and G. R. Luckhurst *Measurements and Interpretation of Flexoelectricity in Physical Properties of Liquid Crystals: Nematics*, page 251 INSPEC, the Institution of Electrical Engineers, London (2001).
15. M. A. Osipov, *J. Phys. Lett* 45, 823 (1984).
16. M. A. Osipov and V. B. Nemtsov, *Sov. Phys. Crystallogr.* 31, 125 (1986).
17. Y. Singh and U. P. Singh, *Phys. Rev. A* 39, 4254 (1989).
18. A. M. Somoza and P. Tarazona, *Molec. Phys.* 72, 911 (1991).
19. J. P. Straley, *Phys. Rev. A* 14, 1835 (1976).
20. M. A. Osipov, *Sov. Phys. JETP* 85, 1167 (1983).
21. A. Ferrarini, *Phys. Rev. E* 64, 021710 (2001).
22. A. V. Zahkarov and R. Y. Dong, *Eur. Phys. J. E* 6, 3 (2001).
23. P. Lebwohl and G. Lasher, *Phys. Rev. A* 6, 426 (1972).

24. S. Dhakal and J. V. Selinger, Phys. Rev. E 81, 031704 (2009).
25. Metropolis and Ulam, 1949.
26. P. Lebowitz and G. Lasher, Phys. Rev. A 6, 426 (1972).
27. R. J. Glauber, the Time-dependent statistics of the Ising Model, J. Math. Phys. 4, 294 (1963).
28. Allen. M. P, Tildesley. D. J, Computer Simulation of Liquids.
29. G. Vertogen, W. H. de Jeu, Thermotropic Liquid Crystals (1987).
30. M. E. J. Newman, Monte Carlo Methods in Statistical Physics (1998).
31. K. P. N. Murthy, Monte Carlo Methods Statistical Physics (2004).
32. S. M. Wong, Computational Methods in Physics and Engineering (1992).

